DETERMINATION OF CREEP PROPERTIES OF ROCK SALT USING MODIFIED POINT LOAD TESTING

Pichit Samsri

A Thesis Submitted in Partial Fulfillment of the Requirements for the

Degree of Master of Engineering in Geotechnology

Suranaree University of Technology

Academic Year 2010

การหาคุณสมบัติของเกลือหินโดยวิธีการทดสอบจุดกดแบบปรับเปลี่ยน

นายพิชิต เสมศรี

วิทยานิพนธ์นี้เป็นส่วนหนึ่งของการศึกษาตามหลักสูตรปริญญาวิศวกรรมศาสตรมหาบัณฑิต
สาขาวิชาเทคโนโลยีธรณี
มหาวิทยาลัยเทคโนโลยีสุรนารี
ปีการศึกษา 2553

DETERMINATION OF CREEP PROPERTIES OF ROCK SALT USING MODIFIED POINT LOAD TESTING

Suranaree University of Technology has approved this thesis submitted in partial fulfillment of the requirements for a Master's Degree.

Thesis Examining Committee

_____

(Asst. Prof. Thara Lekuthai)

Chairperson

_____

(Assoc. Prof. Dr. Kittitep Fuenkajorn)

Member (Thesis Advisor)

_____

(Dr. Prachya Tepnarong)

Member

_____

(Prof. Dr. Sukit Limpijumnong)

Vice Rector for Academic Affairs

_____

(Assoc. Prof. Dr. Vorapot Khompis)

Dean of Institute of Engineering

พิชิต เสมศรี : การหาคุณสมบัติของเกลือหินโดยวิธีการทดสอบจุดกดแบบปรับเปลี่ยน (DETERMINATION OF CREEP PROPERTIES OF ROCK SALT USING MODIFIED POINT LOAD TESTING) อาจารย์ที่ปรึกษา : รองศาสตราจารย์ ดร.กิตติเทพ เฟื่องขจร, 85 หน้า.

วัตถุประสงค์ของงานวิจัยนี้ คือ เพื่อพัฒนาการทดสอบแบบใหม่เพื่อหาคุณสมบัติเชิงเวลาของเกลือหินในห้องปฏิบัติการ การทดสอบจุดกดแบบปรับเปลี่ยนถูกเสนอขึ้นในงานวิจัยนี้เพื่อหาคุณสมบัติเชิงเวลาของหน่วยเกลือหินชั้นกลางและชั้นล่างในหมวดหินมหาสารคาม ตัวอย่างเกลือหินถูกจัดเตรียมเป็นรูปแผ่นวงกลมที่มีเส้นผ่าศูนย์กลาง 48 มม. และ 101 มม. อุปกรณ์ที่ใช้ทดสอบมีลักษณะคล้ายคลึงกับการทดสอบจุดกดแบบดั้งเดิม แต่ต่างกันตรงที่หัวกดได้ถูกตัดเรียบและพื้นที่หน้าตัดเป็นรูปวงกลมแทนที่จะเป็นรูปครึ่งทรงกลม หัวกดจะให้แรงคงที่ในแนวแกนของตัวอย่างหิน การยุบตัวที่เกิดขึ้นในแนวแกนของตัวอย่างหินจะถูกตรวจวัดอย่างต่อเนื่องเป็นเวลา 30 วันหรือจนกระทั่งเกิดการแตกของหิน นอกจากนั้นจะมีการทดสอบการกดแบบวัฏจักรสำหรับจุดกดแบบปรับเปลี่ยนและการทดสอบแรงกดในแกนเดียวด้วย เพื่อหาค่าสัมประสิทธิ์ความยืดหยุ่นที่แท้จริงของเกลือหินภายใต้รูปแบบของการกดที่ต่างกัน ผลการทดสอบจุดกดแบบปรับเปลี่ยนจะวิเคราะห์ด้วยแบบจำลองเชิงตัวเลขเพื่อหาค่าคุณสมบัติความยืดหยุ่นและการคืบของตัวอย่างเกลือหิน โดยสมมติว่าเกลือหินเหล่านั้นมีพฤติกรรมการคืบที่เป็นไปตามกฎของ Burgers ความน่าเชื่อถือของการทดสอบการคืบโดยใช้วิธีจุดกดแบบปรับเปลี่ยนได้ถูกประเมินโดยการเปรียบเทียบผลที่ได้กับการทดสอบการคืบในสามแกนแบบดั้งเดิม ผลจากงานวิจัยระบุว่าค่าสัมประสิทธิ์ความยืดหยุ่นที่วัดได้จากการทดสอบจุดกดแบบปรับเปลี่ยนและการทดสอบแรงกดในแกนเดียวมีค่าสอดคล้องกัน ค่าสัมประสิทธิ์ความหนืดเชิงยืดหยุ่นและความหนืดเชิงพลาสติกที่วัดได้จากการทดสอบการคืบด้วยวิธีจุดกดแบบปรับเปลี่ยน มีค่าประมาณครึ่งหนึ่งของค่าที่วัดได้ด้วยวิธีการทดดสอบการคืบในสามแกนแบบดั้งเดิม ผลจากงานวิจัยบอกเป็นนัยว่าผลที่ได้จากการทดสอบด้วยวิธีจุดกดแบบปรับเปลี่ยนจะให้ค่าการเปลี่ยนรูปในเชิงเวลาของเกลือหินในภาคสนามที่สูงกว่าผลที่ได้จากการทดสอบด้วยวิธีแบบดั้งเดิม

สาขาวิชาเทคโนโลยีธรณี ลายมือชื่อนักศึกษา _____

ปีการศึกษา 2553 ลายมือชื่ออาจารย์ที่ปรึกษา_____

PICHIT SAMSRI : DETERMINATION OF CREEP PROPERTIES OF ROCK SALT USING MODIFIED POINT LOAD TESTING. THESIS ADVISOR : ASSOC. PROF. KITTITEP FUENKAJORN, Ph.D., P.E., 85 PP.

CREEP/POINT LOAD/ROCK SALT/FAILURE/TESTING

The objective of this research is to develop a new testing technique to determine the creep properties of rock salt in the laboratory. A modified point load (MPL) testing technique is proposed to assess the time-dependent properties of the Middle and Lower salt members of the Maha Sarakham formation. The salt specimens are prepared to obtain rock disk specimens with diameters of 48 and 101 mm. The test apparatus is similar to that of conventional point load test, except that the loading points are cut flat to have a circular cross-sectional area instead of a half-spherical shape. The point loading platens apply constant axial loads to the circular disk specimens. The induced axial deformation is monitored for various applied axial stresses up to 30 days or until failure occurs. Cyclic loading is also used for the MPL testing and for the uniaxial compression testing to determine the true elastic modulus of the salt under different loading configurations. Supported by the numerical simulations the MPL test results are used to determine the elastic and creep parameters of the rock salt by assuming that the salt creep behavior follows the Burgers behavior. The reliability of the MPL creep testing technique is assessed by comparing its results with those of the conventional triaxial creep testing. The results indicate that the elastic modulus obtained from the MPL cyclic loading test and the uniaxial compression tests are similar. The visco-elastic and visco-plastic coefficients obtained

from the MPL creep testing are about half of those obtained from the conventional triaxial creep testing. The findings suggest that the MPL test results may predict a greater time-dependent deformation of the in-situ salt than do the conventional testing method.

School of Geotechnology Student's Signature_____

Academic Year 2010 Advisor's Signature_____

ACKNOWLEDGMENTS

I wish to acknowledge the funding support from Suranaree University of Technology (SUT).

I would like to express my sincere thanks to Assoc. Prof. Dr. Kittitep Fuenkajorn, thesis advisor, who gave a critical review and constant encouragement throughout the course of this research. Further appreciation is extended to Asst. Prof. Thara Lekuthai, chairman of School of Geotechnology and Dr. Prachya Tepnarong, School of Geotechnology, Suranaree University of Technology who are members of my examination committee. I am grateful to Pimai Salt Company for donating salt core for testing. Grateful thanks are given to all staffs of Geomechanics Research Unit, Institute of Engineering who supported my work.

Finally, I most gratefully acknowledge my parents and friends for all their supported throughout the period of this research.

Pichit Samsri

TABLE OF CONTENTS

Page

TABLE OF CONTENTS (Continued)

Page

TABLE OF CONTENTS (Continued)

Page

LIST OF TABLES

Table **Page**

LIST OF FIGURES

Figure **Page**

LIST OF FIGURES (Continued)

Figure **Page**

LIST OF FIGURES (Continued)

Figure **Page**

LIST OF FIGURES (Continued)

Figure **Page**

LIST OF SYMBOLS AND ABBREVIATIONS

CPL	=	Conventional point load
D	=	Diameter of rock specimen
d	=	Diameter of loading loint
E	=	Young's modulus
E_1	=	Elastic modulus
E_2	=	Visco-elastic parameter
E_{mpl}	=	Elastic modulus by MPL test
G	=	Shear modulus
I_S	=	Point load strength index
K	=	Bulk modulus
L	=	Specimen length
L/D	=	Length-to-diameter ratio
MPL	=	Modified point load
N	=	Number of loading cycle
P_f	=	Failure load
P_{mpl}	=	Modified point load strength
S	=	Fatigue stress
t	=	Specimen thickness
t/d	=	Specimen thickness-to- diameter of loading point
α	=	Empirical constant
α_E	=	Displacement function

LIST OF SYMBOLS AND ABBREVIATIONS (Continued)

β	=	Empirical constant
δ	=	Axial deformation
ΔP	=	Change in applied stress
$\Delta\delta$	=	Change in vertical of point load platens
$\Delta\delta(t)$	=	Displacement which is a function of time
ε_1	=	Strain in maximum principal stress direction
ε_2	=	Strain in intermediate principal stress direction
ε_3	=	Strain in minimum principal stress direction
ε_V	=	Volumetric strain
γ_{oct}	=	Octahedral shear strain
γ_{oct} (t)	=	Octahedral shear strain which is a function of time
η_1	=	Visco-plastic parameter
η_2	=	Visco-elastic parameter
ν	=	Poisson's ratio
ρ	=	Rock density
σ_1	=	Maximum principal stress (vertical stress)
σ_3	=	Minimum principal stress (horizontal stress)
τ_{oct}	=	Octahedral shear stress

CHAPTER I

INTRODUCTION

1.1 Background and rationale

For nearly a decade, modified point load (MPL) testing has been used to estimate the compressive and tensile strengths and elastic modulus of rock specimens in the laboratory. This method was invented and patented by Suranaree University of Technology. The test apparatus and procedure are intended to be inexpensive and easy, compared to the relevant conventional methods of determining the mechanical properties of rock, such as those given by the International Society for Rock Mechanics (ISRM) and the American Society for Testing and Material (ASTM). Much of the MPL testing practices have been used to determine the elasticity and strengths of soft to medium strong rocks. Test results from time-dependent rocks, such as rock salt, have been rare. In particular application of the point load testing technique to determine the creep or time-dependent properties has never been attempted.

1.2 Research objectives

The objective of this research is to determine the time-dependent properties of rock salt using the modified point load testing technique. This technique is proposed here as an alternative method of determining the time-dependent properties of creeping rock in the laboratory. This is because the point load testing procedure and

sample preparation are quicker and simpler compared to that of the conventional uniaxial and triaxial creep testing. In this research the modified point load tests under various constant axial loads will be performed on circular disks of Maha Sarakham salt. The test apparatus is similar to that of the conventional point load, except that the loading points are cut flat to have a circular cross-sectional area instead of using a half spherical shape (Tepnarong, P., 2006). The axial displacements will be recorded as a function of time and loading magnitudes. The results will be used to calibrate the elastic, visco-elastic and visco-plastic parameters of the rock. It is assumed here that the salt behaviour can be described by Burgers model. Two methods will be employed in the parameter calibration: (1) regression analysis on the linear visco-elastic equation of Burgers model, and (2) numerical simulation using finite difference program (FLAC). Series of conventional triaxial creep tests and cyclic loading tests will also be performed on the salt to determine its elastic and time-dependent properties. The salt properties obtained from the modified point load testing will be compared with those calibrated from the conventional methods. Similarities and discrepancies will be identified. An empirical relation will be developed to correlate the creep properties obtained from the two approaches. Applicability and limitations of the proposed method will be discussed.

1.3 Research methodology

This research consists of six main tasks; literature review, sample preparation, laboratory tests, calibration of Burgers parameters, comparison, and conclusions and thesis writing. The work plan is illustrated in the Figure 1.1.

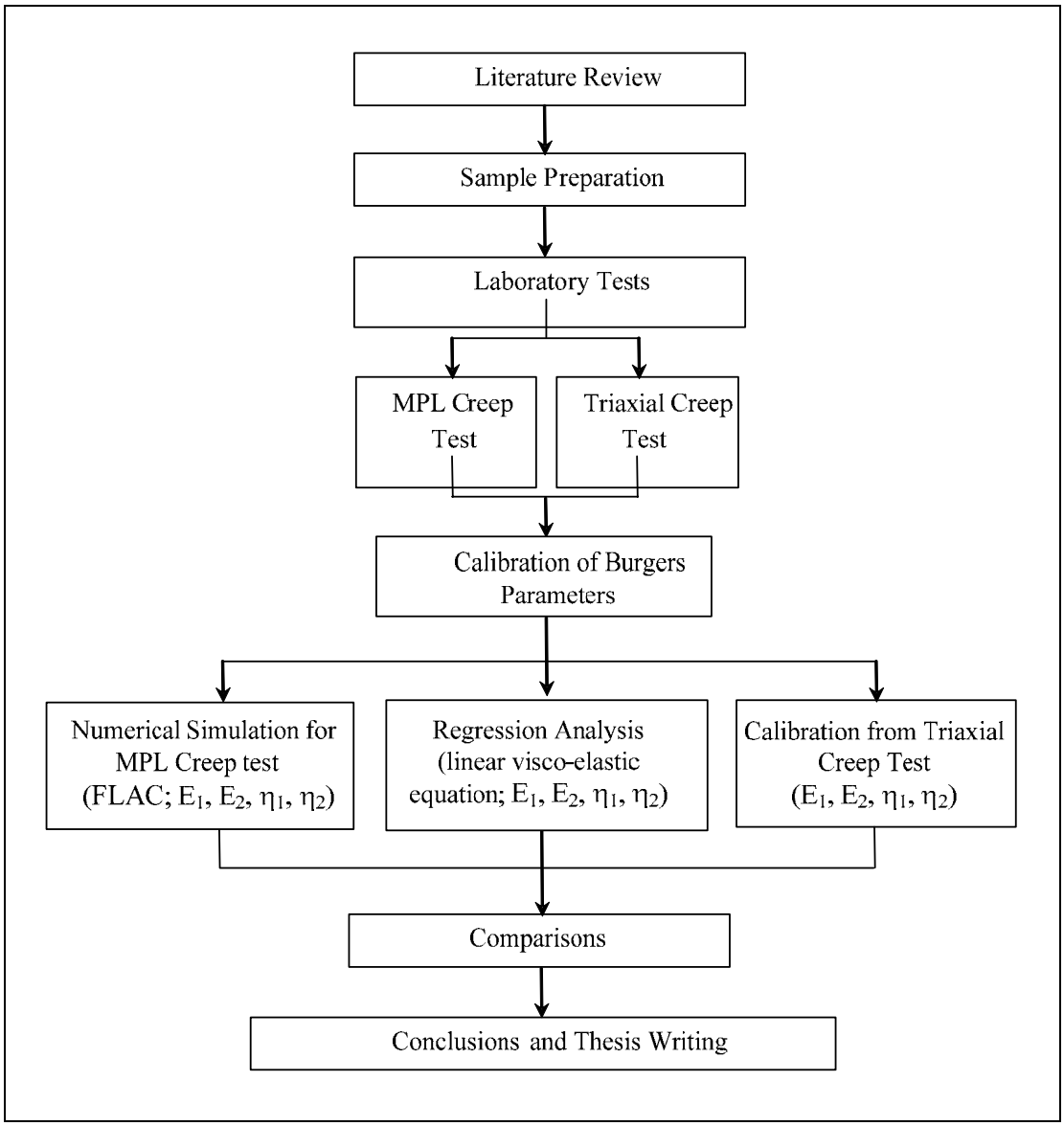

Figure 1.1. Research plan

1.3.1 Literature review

Literature review has been carried out to study the rock salt behaviour and MPL techniques, including theories, test procedure, results, analysis and applications. The sources of information are from journals, technical reports and conference papers.

1.3.2 Sample preparation

Rock samples used here have been obtained from the Middle and Lower Salt members of the Maha Sarakham formation in the northeastern Thailand. The rock salt is relatively pure halite with slight amount (less than 1-2%) of anhydrite, clay minerals and ferrous oxide. The average crystal (grain) size is about 5×5×10 mm^3. Sample preparation is carried out in the laboratory at Suranaree University of Technology.

1.3.3 Laboratory testing

The laboratory tests include uniaxial cyclic loading tests cyclic MPL tests, triaxial creep testing, and MPL creep testing. A series of uniaxial cyclic loading tests is performed on the 48 mm diameter salt core specimens using a SBEL PLT-75 testing machine. The maximum axial stresses vary among specimens about 60% to 100% of the salt compressive strength. The loading frequency is 0.3 Hz. The cyclic MPL tests are performed on salt specimens with thickness-to-loading point diameter ratio (t/d) of 2 and diameter of specimen-to-loading point diameter ratio (D/d) of 2 to 4. The MPL loading points used in this study are 10 to 30 mm in diameter. The triaxial creep test determines visco-plastic and visco-elastic parameters of the salt specimens under confined condition. The time-related parameters are monitored, recorded and analyzed. The mathematical solution is derived to correlate the elastic modulus of rock salt specimens. The MPL creep test determines the time-dependent properties of the salt under isothermal condition. The results are used to calibrate the visco-plastic and visco-elastic parameters coefficient of the salt. The tests are performed on salt specimens with thickness-to-loading point diameter ratio (t/d)

of 2, with diameter of specimen-to-loading point diameter ratios (D/d) of 2 and 4. Over 30 specimens are used for this study

1.3.4 Calibration of Burgers parameters

The results are used to calibrate the elastic, visco-elastic and visco-plastic parameters of the rock. It is assumed here that the salt behaviour can be described by the Burgers model. The regression analysis on the linear visco-elastic equation of Burgers model and the finite difference code (FLAC) is employed in the calibration. Series of conventional triaxial creep tests and cyclic loading tests are also performed on the salt to determine its elastic and time-dependent properties.

1.3.5 Comparisons

The elastic and time-dependent parameters from the modified point load testing results will be compared with those calibrated from the conventional methods. Similarity and discrepancy are examined. Applicability of the MPL on rock creep determination are discussed.

1.3.6 Conclusions and thesis writing

All research activities, methods, and results are documented and complied in the thesis. The research findings are published in the conference proceedings or journals.

1.4 Scope and limitations

The scope and limitations of the research include as follows.

1. The laboratory tests include uniaxial cyclic loading tests cyclic modified point load tests, modified point load creep testing, and triaxial creep testing.

2. The tests will use rock salt from the middle and lower units of the Maha Sarakham Formation in northeastern Thailand.

3. The effects of loading rate and temperature are not considered. All tests are conducted at room temperature.

4. The time-dependent properties parameters will be determined based on the Burgers model.

5. FLAC and regression analysis on the linear visco-elastic equation of Burgers model will be employed in the calibration.

6. Comparison of the results from MPL tests and conventional method will be made.

7. The research findings will be published in conference paper or journal.

1.5 Thesis contents

This first chapter introduces the thesis by briefly describing the rationale and background and identifying the research objectives. The third section describes scope and limitations. The fourth section identifies the research methodology. The fifth section gives a chapter by chapter overview of the contents of this thesis.

The second chapter summarizes results of the literature review. Chapter three describes samples preparation. The methods and results of the laboratory testing are described in chapter four. The results from calibration are compared in chapter five. Chapter six provides the conclusion and recommendations for future research studies.

CHAPTER II

LITERATURE REVIEW

2.1 Introduction

This chapter summarizes the results of literature review carried out to improve an understanding of rock salt behaviour. The topics reviewed here include effect of grain size, inclusions, and modified point load test.

2.2 Salt behavior

Researchers from the field of material sciences believe that rock salt behaviour shows many similarities with that of various metals and ceramics (Chokski and Langdon, 1991; Munson and Wawersik, 1993). However, because alkali halides are ionic materials, there are some important differences in their behavior. Aubertin et al. (1992; 1993; 1998; 1999) conclude that the rock salt behavior should be brittle-to ductile materials or elastic-plastic behavior. This also agrees with the finding by Fuenkajorn and Daemen (1988); Fokker and Kenter (1994); Fokker (1995; 1998).

Jeremic (1994) discusses the mechanical characteristics of the salt. They are divided into three characteristics: the elastic, the elastic-plastic, and the plastic behavior. The elastic behavior of rock salt is assumed to be linearly elastic with brittle failure. The rock salt is observed as linear elastic only for a low magnitude of loading. The range of linear elastic mainly depends on the content of elastic strain and can be used to formulate the modulus of elasticity. Normally, the modulus of elasticity

of rock salt is relatively low. The elastic and plastic behavior of rock salt can be investigated from the rock salt specimen. The confined rock salt specimen at the beginning of incremental loading shows linear elastic deformation but with further load increases the plastic behavior is induced, which continues until yield failure. Elastic deformation and plastic deformation are considered as separated modes of deformability in the great majority of cases. The salt material simultaneously exhibits both elastic strain and plastic strain. The difference between elastic behavior and plastic behavior is that elastic deformation is temporary (recoverable) and plastic deformation is permanent (irrecoverable). The degree of permanent deformation depends on the ratio of plastic strain to total strain. The elastic and plastic deformation can also be observed by short-term loading, but at higher load magnitude. The plastic behavior of rock salt does not occur if the applied stress is less than the yield stress. The rock salt is deformed continually if the high stress rate is still applied and is more than the yield stress. Increasing the load to exceed the strain limit of the rock salt beyond its strength causes it to fail. The deformation of 16 rocks salt by the increase of temperature can also result in the transition of brittle-to-ductile behavior.

The time-dependent deformation (or creep) is the process at which the rock can continue deformation without changing stress. The creep strain seldom can be recovery fully when loads are removed, thus it is largely plastic deformation. Creep deformation occurs in three different phases, as shown in Figure 2.1, which relatively represents a model of salt properties undergoing creep deformation due to the sustained constant load. Upon application of a constant force on the rock salt, an instantaneous elastic strain (ε_e) is induced. The elastic strain is followed by a primary or transient strain, shown as Region I. Region II, characterized by an almost constant

slope in the diagram, corresponds to secondary or steady state creep. Tertiary or accelerating creep leading to rather sudden failure is shown in Region III. Laboratory investigations show that removal of applied load in Region I at point L will cause the strain to fall rapidly to the M level and then asymptotically back to zero at N. The distance LM is equal to the instantaneous strain ε_e. No permanent strain is induced here. If the removal of stress takes place in the steady-state phase the permanent strain (ε_p) will occur. From the stability point of view, salt structure deformations after constant load removal have only academic significance, since the stresses imposed underground due to mining operations are irreversible. The behavior of the salts with time-dependent deformation under constant load is characterized as a visco-elastic and visco-plastic phenomenon. Under these conditions the strain criteria are superior to the strength criteria for design purposes, because failure of most salt pillars occurs during accelerated or tertiary phase of creep, due to the almost constant applied load. The dimensions of a pillar in visco-elastic and visco-plastic rock should be established on the basis of a prediction of its long-term strain, to guard against adequate safety factor accelerating creep (Fuenkajorn, K., and Daemen, J.J.K., 1988; Dusseault and Fordham, 1993; Jeremic, 1994; Knowles et al., 1998).

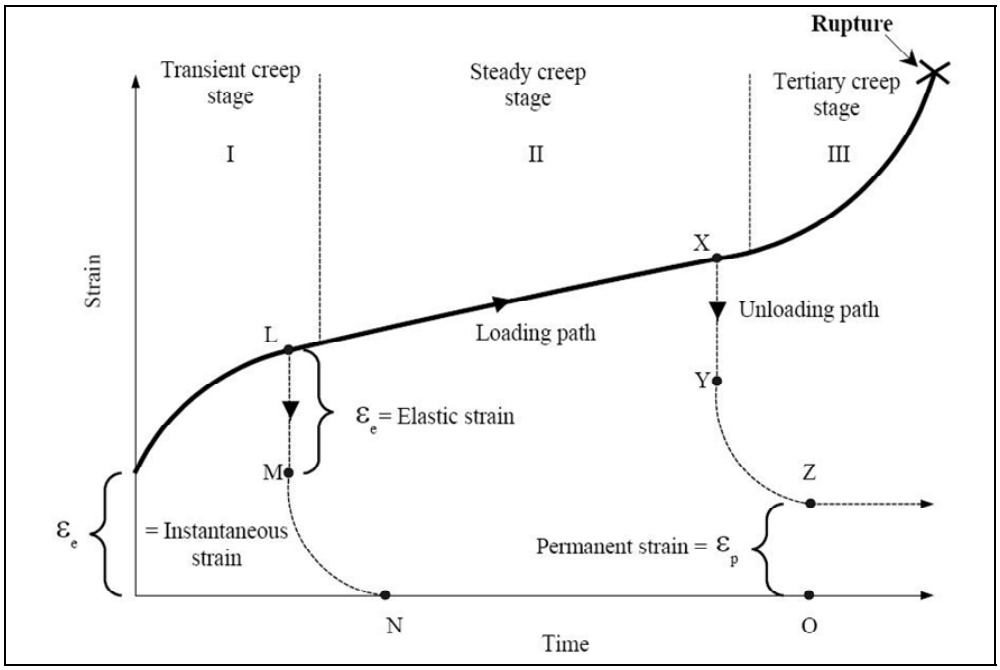

Figure 2.1 The typical deformation as a function of time of creep materials (modified from Jeremic, 1994).

2.3 Effect of grain size and inclusions

The effects of grain size on the creep behavior and strength of rock salt in laboratory and field conditions are described by Fokker (1998). The average grain size of salt visually observed from the core and post-failure specimens is 5 mm × 10 mm × 10 mm. It is concluded that the large size of the salt crystals increases the effect of the crystallographic features (i.e. cleavage planes) on the mechanics of deformation and failure of the samples. This also agrees with the finding by Aubertin (1996). The dislocations and plastic flows in single crystals of halite are studied by several researchers (Franssen and Spiers, 1990; Raj and Pharr, 1992; Senseny et al., 1992; Wanten et al., 1996). They conclude that the shear strength and deformation of halite crystals are orientation-dependent. The small size of the sample may not provide good

representative test results. This also reflects on the specifications by ASTM (ASTM D2664, D2938 and D3967). The ASTM standard methods specify that to minimize the effect of grain size the sample diameter should be at least ten times the average grain size.

Inclusions and impurities in salt have an effect on to the creep deformation and strength of salt. The degree of impurity is varying for different scales of the rock salt. On a small scale, such as for laboratory specimens, the impurities of salt involve ferruginous inclusions and thin clay seams along grain boundaries or bedding planes. The impurities distribute uniformly in the salt may affect the strength of rock salt. This can decrease the creep deformation and strength of rock salt. These phenomena have been reported by Franssen and Spiers (1990); Raj and Pharr (1992); Senseny et al. (1992) as well.

2.4 Constitutive models

Garcia and Estrada (1998) studied correlation between creep tests and variable deviator stress tests in rock salt. The study had as main objective research a method that provided the best selection of samples to develop creep tests and reduce the number of tests, follow this way the test is quicker and cheaper. The current study describes the constitutive equation that reproduces mechanical behaviors in the quick triaxial test and shows the results of the correlation with creep tests. The constitutive equation was intended to reproduce the graphs strain-time and strain-stress of each core. The equation to calculate the distortional strain has as a base the analogical Burger's model subject to deviator stress variables.

$$\varepsilon_B = \varepsilon_M + \varepsilon_K \tag{2.1}$$

from the Burger's model: For Maxwell's model:

$$\varepsilon_B \equiv \varepsilon_M + \varepsilon_K \equiv \frac{\sigma_R}{2G_M} \oplus \int \frac{\sigma_A}{2\nu_M} \tag{2.2}$$

if $\sigma_B = \sigma_M = \sigma_R = \sigma_A = mt$, so if replace G_M by $E_M / (2(1+\mu_M))$ we obtain the follow equation:

$$\varepsilon_M = mt\left[\frac{1 \oplus \mu_M}{E_M} \oplus \frac{t}{4\nu_M}\right] \tag{2.3}$$

where m is the slope in each graphic the tangent line creep, t is time, and $\oplus$ is propositional logic symbol, such as the statement $A \oplus B$ is true when either A or B, but not both, are true. For Kelvin's model:

$$\sigma_B = \sigma_M = \sigma_K = mt \tag{2.4}$$

and

$$\sigma_K = \sigma_R \oplus \sigma_A = \varepsilon_R 2G_K \oplus \varepsilon 2\nu_K \tag{2.5}$$

if $\lambda = G_K / \nu_K$, the follow differential equation is obtained:

$$\left(d\varepsilon_K / dt\right) + \lambda\varepsilon_K = \sigma_K / 2\nu_K \tag{2.6}$$

if σ_K = mt and $G_K = E_K / (2(1+\mu_K))$, we obtain:

$$\varepsilon_K = [\, m(1+\mu_K)/E_K\,][\, t+(2\nu_K(1+\mu_K)/E_K)(e^{-\lambda t}-1)] \tag{2.7}$$

finally if we substitute Equations (2.3) and (2.7) into (2.1) the final constitutive equation that allow analysis the distortional strain other material under deviator stress is:

$$\varepsilon_B = mt * [(1+\mu_M)/E_M + t/4\nu_M] + [m(1+\mu_K)/E_K] * [t+(2\nu_K(1+\mu_K)/E_K) * (e^{-\lambda t}-1)] \tag{2.8}$$

Wang (2004) studied a new constitutive creep-damage model for salt rock established by means of application of damage and a concept of "damage accelerating limit" into Carter's creep model. Verification of the model is carried out based on the creep tests for salt rock. The results showed that the constitutive model not only gave a faithful representation of the creep-damage behaviour for salt rock under high stress, but also described efficiently the primary and stationary creep at low stress. Beyond the damage accelerating limit, the tertiary creep will occur, which influences strongly the damage evolution and creep.

$$\varepsilon = \varepsilon_t + \varepsilon_s + \varepsilon_d \tag{2.9}$$

where ε is total creep, ε_t is transient creep, ε_s is steady creep (Carter's creep model), and ε_d is creep induced by damage.

$$\varepsilon_t = \frac{\sigma}{C_1} \cdot \left[1 - \exp\left(-\frac{G}{C_2} t \right) \right] \tag{2.10}$$

$$\varepsilon_s = A_1 \cdot \exp\left(-\frac{Q_1}{RT} \right) \cdot \sigma^n \cdot t \tag{2.11}$$

$$\varepsilon_d = A_2 \cdot \exp\left(-\frac{Q_2}{RT} \right) \cdot \left(\frac{\sigma}{1 - D} \right)^n \cdot t \tag{2.12}$$

where C_1, C_2, A_1, and A_2 are material coefficients of the Carter's creep model, n is the power index, G is shear modulus, Q_1 and Q_2 are effective activation energy, σ is stress carried by material, t is time load lasts, R is universal gas thermomechanical constant, T is absolute Kelvin temperature in K, and D is damage factor ($0 \leq D < 1$). Furthermore, no great variation of the parameters describing the creep-damage behavior by variant sorts of salt rock and by different test conditions was found. Therefore, the application range of the model is wide. Finally, some parameters studied were carried out and the essential characteristics of the model were investigated.

2.5 Modified point load tests

Tepnarong, P., (2001) proposes a modified point load testing method to correlate the results with the uniaxial compressive strength (UCS) and tensile strength of intact rocks. The primary objective of the research is to develop the inexpensive and reliable rock testing method for use in field and laboratory. The test apparatus is similar to the conventional point load (CPL), except that the loading points are cut flat to have a circular cross-section area instead of using a half-spherical shape.

To derive a new solution, finite element analyses and laboratory experiments were carried out. The simulation results suggest that the applied stress required to fail the MPL specimen increases logarithmically as the specimen thickness or diameter increases. The MPL tests, CPL tests, UCS tests and Brazilian tension tests were performed on Saraburi marble under a variety of sizes and shapes. The UCS test results indicated that the strengths decreased with increased the length-to-diameter ratio. The test results can be postulated that the MPL strength can be correlated with the compressive strength when the MPL specimens are relatively thin, and should be an indicator of the tensile strength when the specimens are significantly larger than the diameter of the loading points. Predictive capability of the MPL and CPL techniques were assessed. Extrapolation of the test results suggested that the MPL results predicted the UCS of the rock specimens better than the CPL testing. The tensile strength predicted by the MPL also agreed reasonably well with the Brazilian tensile strength of the rock.

Tepnarong, P., (2006) proposes the modified point load testing technique to determine the elastic modulus and triaxial compressive strength of intact rocks. The loading platens are made of harden steel and have diameter (d) varying from 5, 10, 15, 20, 25, to 30 mm. The rock specimens tested were marble, basalt, sandstone, granite and rock salt. Basic characterization tests were first performed to obtain elastic and strength properties of the rock specimen under standard testing methods (ASTM). The MPL specimens were prepared to have nominal diameters (D) ranging from 38 mm to 100 mm, with thickness varying from 18 mm to 63 mm. Testing on these circular disk specimens was a precursory step to the application on irregular-shaped specimens. The load was applied along the specimen axis while monitoring the increased of the

load and vertical displacement until failure. Finite element analyses were performed to determine the stress and deformation of the MPL specimens under various D/d and t/d ratios. The numerical results were also used to develop the relationship between the load increases (ΔP) and the rock deformation ($\Delta\delta$) between the loading platens. The MPL testing predicts the intact rock elastic modulus (E_{mpl}) by using an equation: $E_{mpl} = (t/\alpha_E) \cdot (\Delta P/\Delta\delta)$, where t represents the specimen thickness and α_E is the displacement function derived from numerical simulation. The elastic modulus predicted by MPL testing agrees reasonably well with those obtained from the standard uniaxial compressive tests. The predicted E_{mpl} values show significantly high standard deviation caused by high intrinsic variability of the rock fabric. This effect is enhanced by the small size of the loading area of the MPL specimens, as compared to the specimen size used in standard test methods.

The results of the numerical simulation were used to determine the minimum principal stress (σ_3) at failure corresponding to the maximum applied principal stress (σ_1). A simple relation can therefore be developed between σ_1/σ_3 ratio, Poisson's ratio (ν) and diameter ratio (D/d) to estimate the triaxial compressive strengths of the rock specimens: $\sigma_1/\sigma_3 = 2[(\nu/(1-\nu))(1-(d/D)^2)]^{-1}$. The MPL test results from specimens with various D/d ratios can provide σ_1 and σ_3 at failure by assuming that $\nu = 0.25$ and that failure mode follows Coulomb criterion. The MPL predicted triaxial strengths agree very well with the triaxial strength obtained from the standard triaxial testing (ASTM). The discrepancy is about 2-3% which may be due to the assumed Poisson's ratio of 2.5, and due to the assumption used in the determination of σ_3 at failure. In summary, even through slight discrepancies remain in the application of MPL results to determine the elastic modulus and triaxial compressive strength of

intact rocks, this approach of predicting the rock properties shows a good potential and seems promising considering the low cost of testing technique and ease of sample preparation.

CHAPTER III

SAMPLE PREPARATION

3.1 Introduction

This chapter describes the rock salt sample preparation procedure to be used in the uniaxial cyclic loading tests, triaxial creep tests, cyclic MPL tests, and MPL creep tests.

3.2 Sample preparation

The salt specimens tested here are obtained from the Middle and Lower members of the Maha Sarakham formation in the northeastern Thailand. The rock salt is relatively pure halite with slight amount (less than 1-2%) of anhydrite, clay minerals and ferrous oxide. The average crystal (grain) size is about 5×5×5 mm^3. Warren (1999) gave detailed descriptions of the salt and geology of the basin. Sample preparation is conducted in laboratory facility at the Suranaree University of Technology. The specimens are core, cut and ground. Sample preparation followed the ASTM (D4543-08) standard practice as much as practical. The nominal sizes of specimen that are shown in Table 3.1. Tables 3.2 through 3.5 show the summary of salt specimen dimension prepared for each test type. Five specimens prepared for the uniaxial cyclic loading tests have 48 mm in diameter (Figure 3.1). The ratio of specimen length to specimen diameter (L/D) is 2.5. Ten specimens prepared for cyclic MPL tests (Figure 3.2). The MPL loading platen used in this study is 25 mm in

diameter. The specimen thickness to loading platen diameter (t/d) ratio is 2. The ratios of specimen diameter to loading platen diameter (D/d) are 2 and 4. Fivespecimens prepared for triaxial creep tests with diameter 54 mm (Figure 3.3) and specimen length to specimen diameter (L/D) ratio is 2.0. Ten specimens prepared for MPL creep tests (Figure 3.4). The specimen thickness to loading platen diameter (t/d) ratios is 2. The ratios of specimen diameter to loading platen diameter (D/d) are 2 and 4.

Table 3.1 Nominal dimension of specimens for difference tests.

Methods	L/d ratio	D/d ratio	Nominal Diameter (mm)	Nominal Length (mm)	Number of Specimens
Uniaxial cyclic loading test	2.5	-	48	120	5
MPL cyclic loading test	2.0	2.0	48	50	5
	2.0	4.0	101	50	5
Triaxial creep test	2.0	-	54	108	5
MPL creep test	2.0	2.0	48	50	5
	2.0	4.0	101	50	5

Table 3.2 Salt specimens prepared for uniaxial cyclic loading tests.

Specimen Number	Depth (m)	Average Diameter (mm)	Average Length (mm)	Density (g/cc)	L/D Ratio
MS-UCL-01	340.20-340.38	47.89	123.12	2.14	2.57
MS-UCL-02	340.40-340.55	47.89	124.79	2.15	2.61
MS-UCL-03	341.07-341.30	47.73	123.27	2.14	2.58
MS-UCL-04	341.42-341.59	47.95	123.79	2.15	2.58
MS-UCL-05	341.63-341.79	47.70	122.35	2.16	2.56

Table 3.3 Salt specimens prepared for cyclic MPL tests.

Specimen Number	Depth (m)	D/d Ratio	Average Diameter (mm)	Average Thickness (mm)	Density (g/cc)
MS-MPC2-01	365.31-365.40	2	47.7	51.4	2.16
MS-MPC2-02	365.44-365.50		47.7	53.1	2.15
MS-MPC2-03	365.21-365.30		47.6	54.0	2.14
MS-MPC2-04	366.20-366.33		47.9	53.5	2.15
MS-MPC2-05	366.35-366.44		47.7	50.1	2.14
MS-MPC4-01	220.05-220.20	4	100.8	52.2	2.14
MS-MPC4-02	220.23-220.29		100.8	51.5	2.15
MS-MPC4-03	222.25-222.42		100.8	51.7	2.16
MS-MPC4-04	222.51-222.63		100.8	51.8	2.15
MS-MPC4-05	224.15-224.24		100.83	51.5	2.15

Table 3.4 Salt specimens prepared for triaxial creep tests.

Specimen Number	Depth (m)	Average Diameter (mm)	Average Length (mm)	Density (g/cc)	L/D Ratio
MS-TCR-01	250.21-250.42	54.2	110.5	2.17	2.0
MS-TCR-02	250.45-250.59	54.5	109.5	2.15	2.0
MS-TCR-03	252.36-252.54	54.6	109.2	2.17	2.0
MS-TCR-04	251.20-251.39	54.5	111.5	2.16	2.0
MS-TCR-05	255.67-256.02	54.4	111.4	2.17	2.0

Table 3.5 Salt specimens prepared for MPL creep tests.

Specimen Number	Depth (m)	D/d Ratio	Average Diameter (mm)	Average Thickness (mm)	Density (g/cc)
MS-MCR2-01	345.15-345.28	2	47.7	49.3	2.16
MS-MCR2-02	346.21-346.29		47.7	49.9	2.15
MS-MCR2-03	345.35-345.40		46.7	50.3	2.21
MS-MCR2-04	346.42-346.51		46.7	49.7	2.17
MS-MCR2-05	346.55-346.64		47.3	49.2	2.16
MS-MCR4-01	208.15-209.23	4	101.6	51.8	2.15
MS-MCR4-02	209.45-209.54		101.6	51.6	2.17
MS-MCR4-03	209.61-209.70		101.5	51.4	2.19
MS-MCR4-04	208.05-208.12		101.4	53.6	2.15
MS-MCR4-05	211.37-211.52		101.5	52.9	2.16

Figure 3.1 Some rock salt specimens prepared for uniaxial cyclic loading tests.

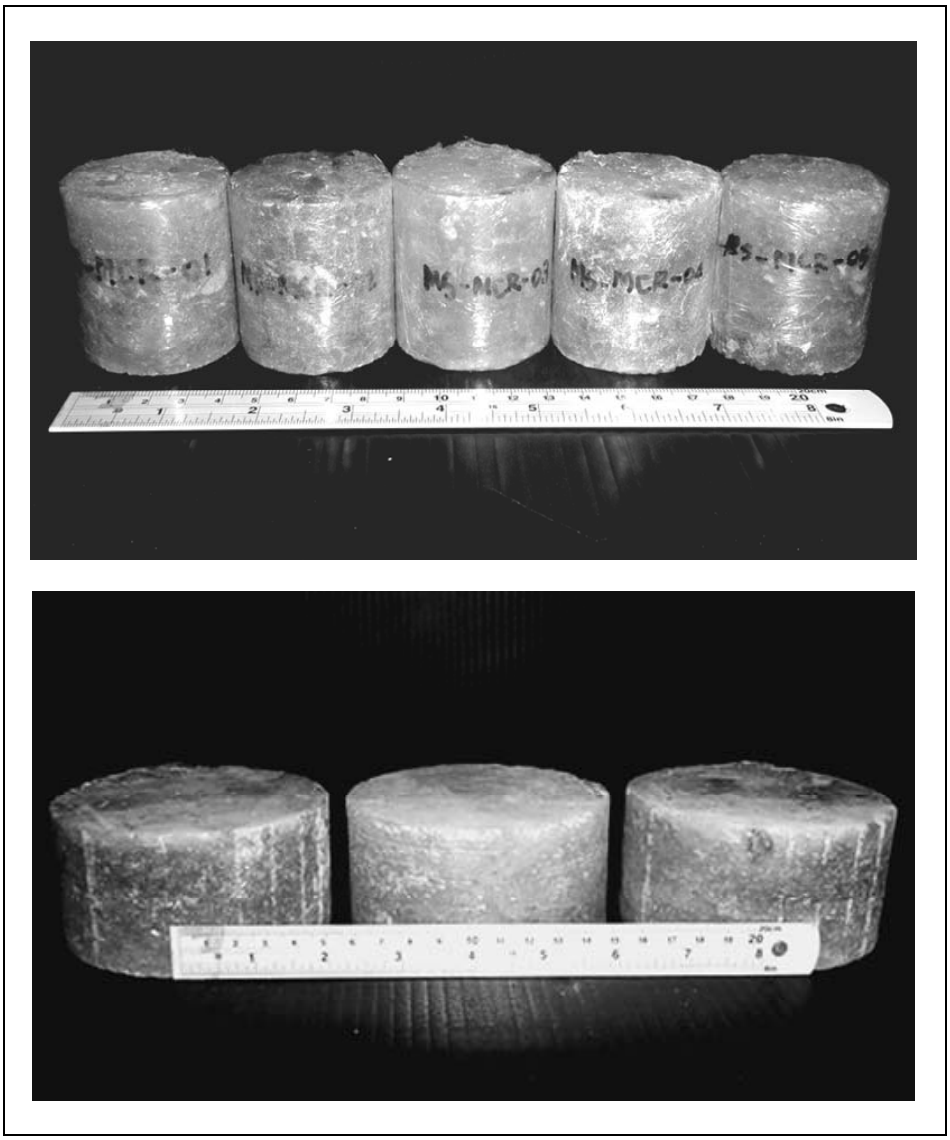

Figure 3.2 Some rock salt specimens prepared for cyclic MPL tests with D/d = 2 (top) and D/d = 4 (bottom).

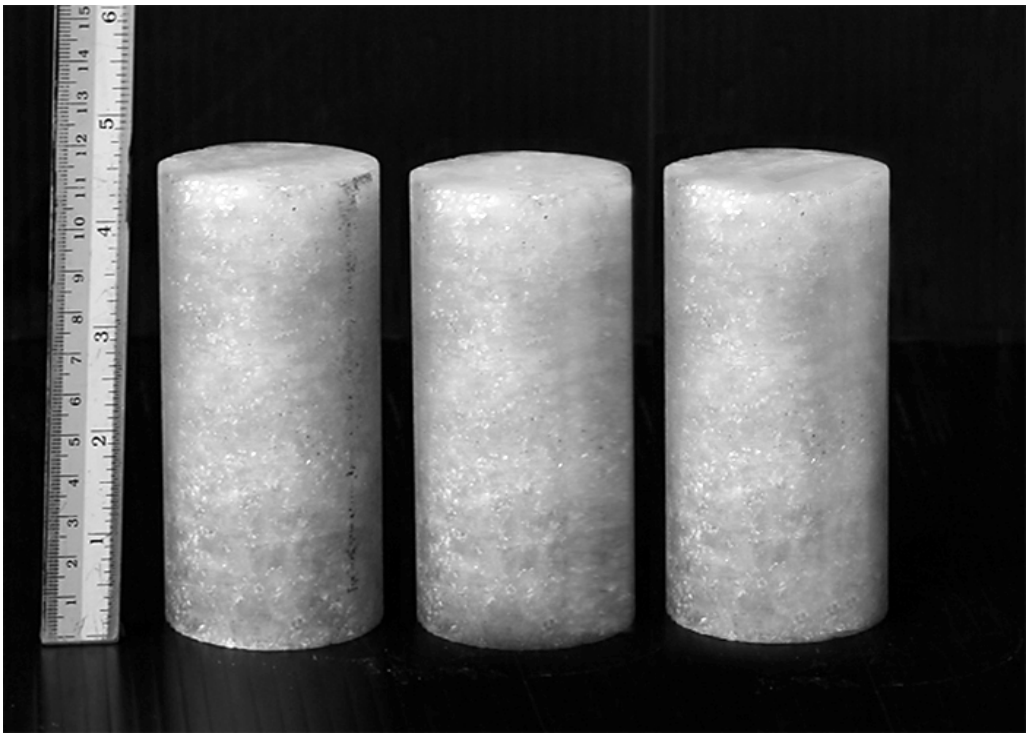

Figure 3.3 Some rock salt specimens prepared for triaxial creep tests L/D = 2.0

Figure 3.4 Some rock salt specimens prepared for MPL creep tests with D/d = 2 (top) and D/d = 4 (bottom).

CHAPTER IV

LABORATORY TESTING

4.1 Introduction

The objective of the laboratory testing is to determine the time-dependent properties of the Maha Sarakham salt. This chapter describes the method and results of the uniaxial cyclic loading tests, cyclic MPL tests, triaxial creep tests, and MPL creep testing.

4.2 Uniaxial cyclic loading tests

4.2.1 Test method

The objective of this test is to determine the true elastic modulus of the salt. A series of uniaxial cyclic loading tests have been performed on the 48 mm diameter salt core specimens using a SBEL PLT-75 testing machine (Figure 4.1). The tests are performed by symmetrically increasing and decreasing axial load on the test specimens. The test has been performed at room temperature. Figure 4.2 shows post-test specimens from the uniaxial cyclic loading tests. The magnitudes of the axial load in each cycle are in the range of 60% to 100% of the strength while the minimum axial stress is maintained constant at 0.1 MPa for all specimens. This small minimum stress is required to ensure that the ends of the specimen remain in contact with the loading platens during the test. The loading frequency is about 0.3 Hz. A total of five specimens have been tested.

4.2.2 Test results

The uniaxial cyclic loading tests results of the rock salt are summarized in Table 4.1. The maximum axial stresses vary among specimens from 16.4 MPa to 18.3 MPa (about 60% to 100% of the compressive strength). The strength value is determined by the conventional uniaxial compressive strength test (Figure 4.3). The axial stress-strain curves measured during loading and unloading are given in Figure 4.4.

4.2.3 Discussions

The post-test specimens show shear failure. The fracture occurs along the crystal grain boundary with a little increasing in volume. This is different from the fracture occurred in the test with higher failure stress. The failure planes make the angles of 0 to 20 degrees with the core axis.

The stress-strain curves can be used to determine the elastic modulus. It is calculated from the series of unloading curves as a function of loading cycles for a loading frequency of 0.3 Hz. The elastic modulus is calculated by the following equation:

$$E = (\Delta\sigma_{axial}) / (\Delta\varepsilon_{axial}) \quad (4.1)$$

where $\Delta\sigma_{axial}$ is the differential value of maximum and minimum stresses and $\Delta\varepsilon_{axial}$ is the differential strains in each cycle. The calculated elastic modulus values range from 10.3 GPa to 21.1 GPa (Table 4.2). Figure 4.5 shows the elastic modulus values calculated from the series of unloading curves as a function of loading cycles. It can be seen the elastic modulus decreases as the number of loading cycles increases. The accumulated axial strain, fatigue stress (S) and time are monitored during loading.

Figure 4.6 illustrates the decrease of the failure (fatigue) stress as the number of loading cycle (N) increases, which can be represented by a power equation:

$$S = 20.63\ N^{(-0.033)}\ \text{MPa} \tag{4.2}$$

where S is maximum stress and N is number of loading cycle. The behavior is similar to those obtained elsewhere for other geologic materials (Costin and Holcomb, 1981; Thoms and Gehle, 1982; Passaris, 1982; Bagde and Petros, 2004, 2005). Figure 4.7 shows the axial strain–time curves compiled from the unloading cycles. The axial strain at failure decreases with increases the maximum stress.The S-N curve and the axial strain-time curves are close to those tested by Fuenkajorn and Phueakphum (2010).

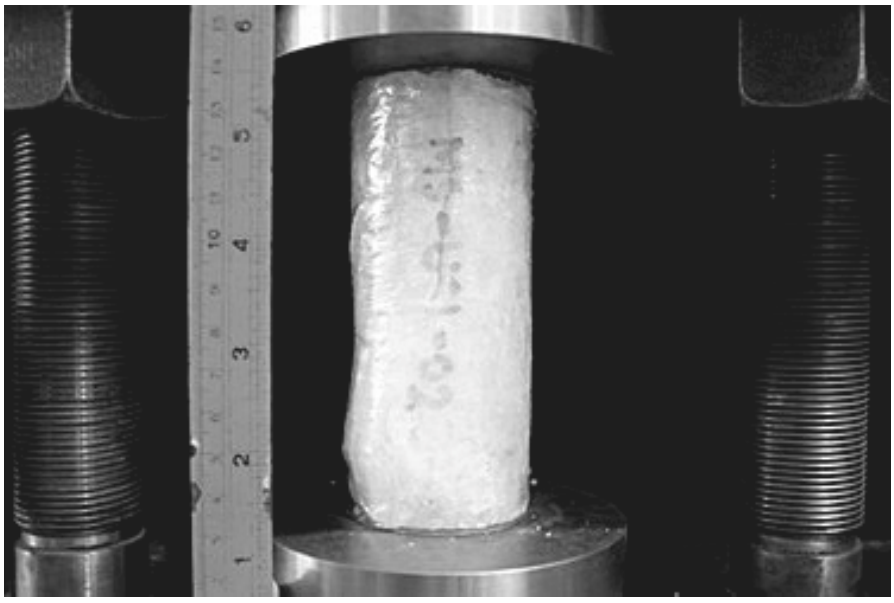

Figure 4.1 Salt specimen placed in the SBEL PLT-75 testing machine for uniaxial cyclic loading test.

Figure 4.2 Examples of post-test specimens from the uniaxial cyclic loading test.

Table 4.1 Summary result of uniaxial cyclic loading tests.

Specimen No.	Depth (m)	Average Diameter (mm)	Average Length (mm)	Density (g/cc)	Maximum Stress (MPa)	Number of Loading Cycles at Failure
01	340.20-340.38	47.89	123.12	2.14	20.8	1
02	340.40-340.55	47.89	124.79	2.15	17.8	218
03	341.07-341.30	47.73	123.27	2.14	17.3	292
04	341.42-341.59	47.95	123.79	2.15	18.3	18
05	341.63-341.79	47.70	122.35	2.16	16.4	501

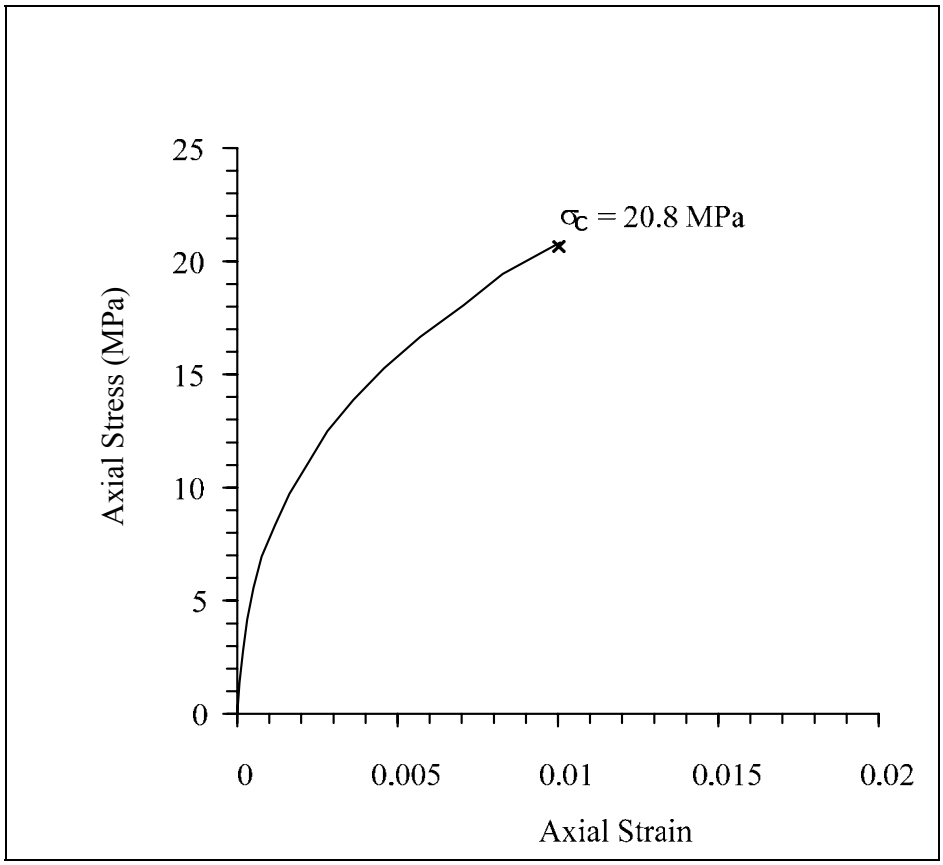

Figure 4.3 Result of uniaxial compressive strength test.

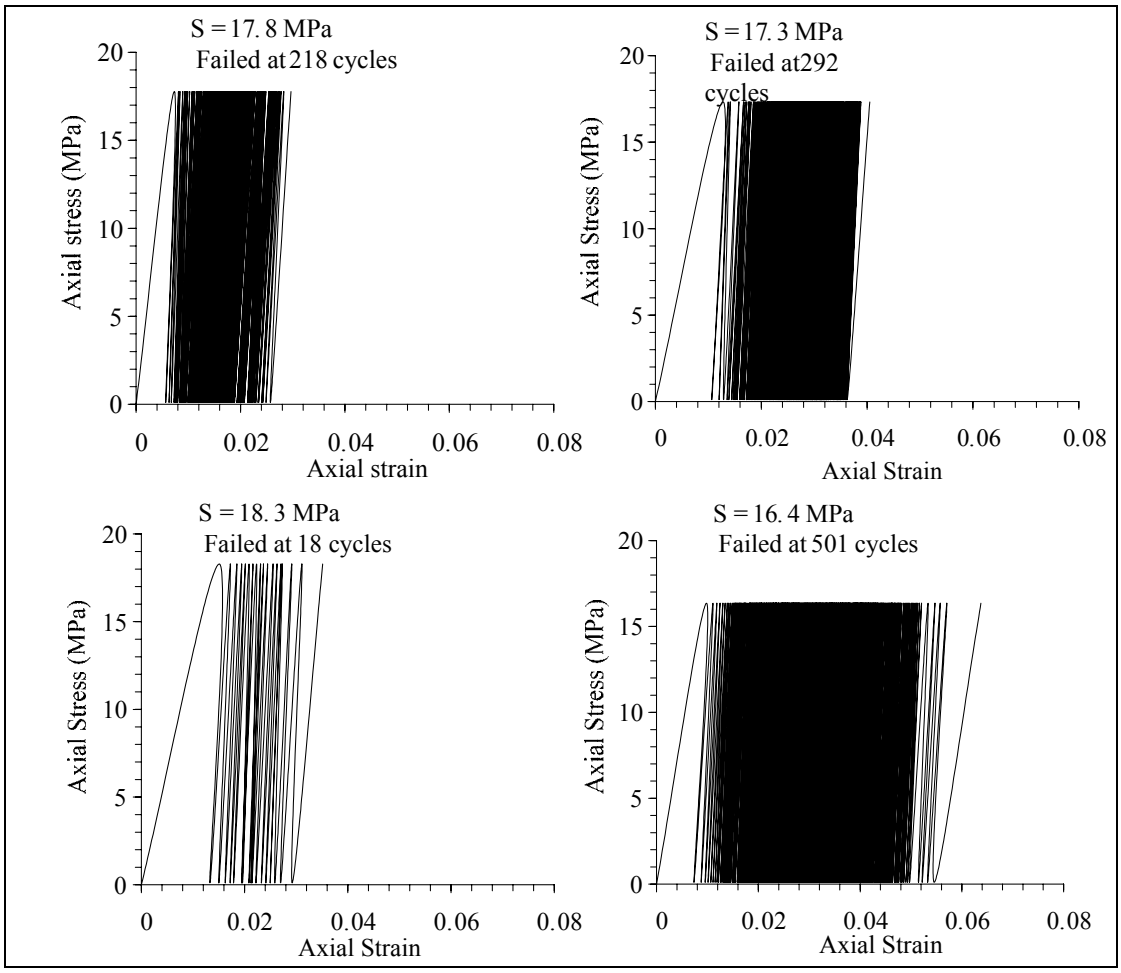

Figure 4.4 Uniaxial cyclic loading test results. Axial stress plotted as a function of axial strain.

Table 4.2 Results of elastic modulus calculated from uniaxial cyclic loading tests.

Specimen No.	Depth (m)	Density (g/cc)	Maximum Stress (MPa)	Number of Cycles	Elastic Modulus (GPa)
01	340.20-340.38	2.14	20.8	1	21.1
02	340.40-340.55	2.15	17.8	218	11.2
03	341.07-341.30	2.14	17.3	292	10.5
04	341.42-341.59	2.16	18.3	18	15.0
05	341.63-341.79	2.15	16.4	501	10.3
Mean±S.D.					13.6±4.6

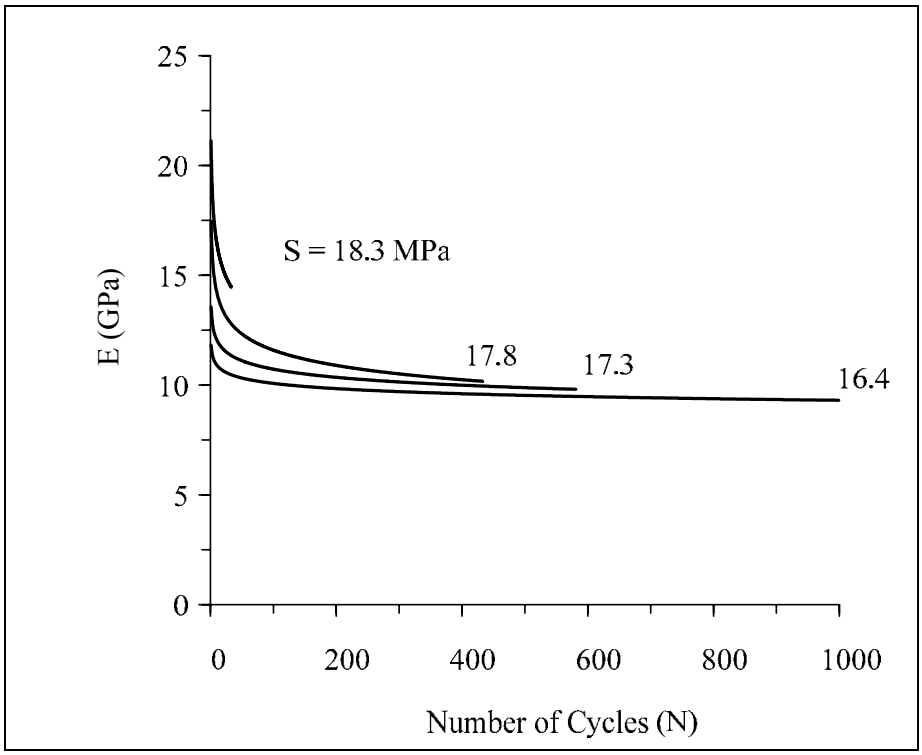

Figure 4.5 Elastic modulus plotted as a function of number of loading cycles at failure (N).

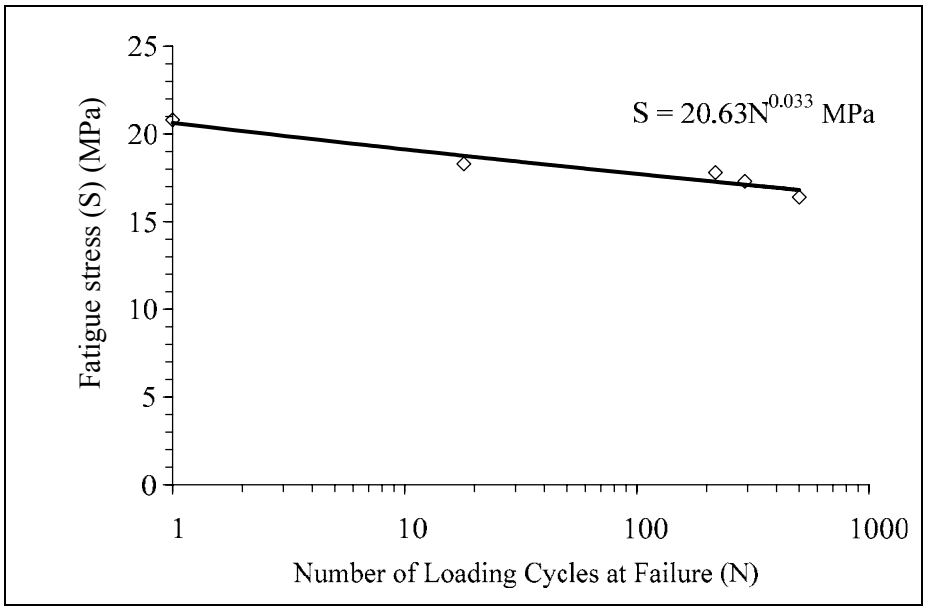

Figure 4.6 Failure stress (S) plotted as a function of number of loading cycles at failure (N).

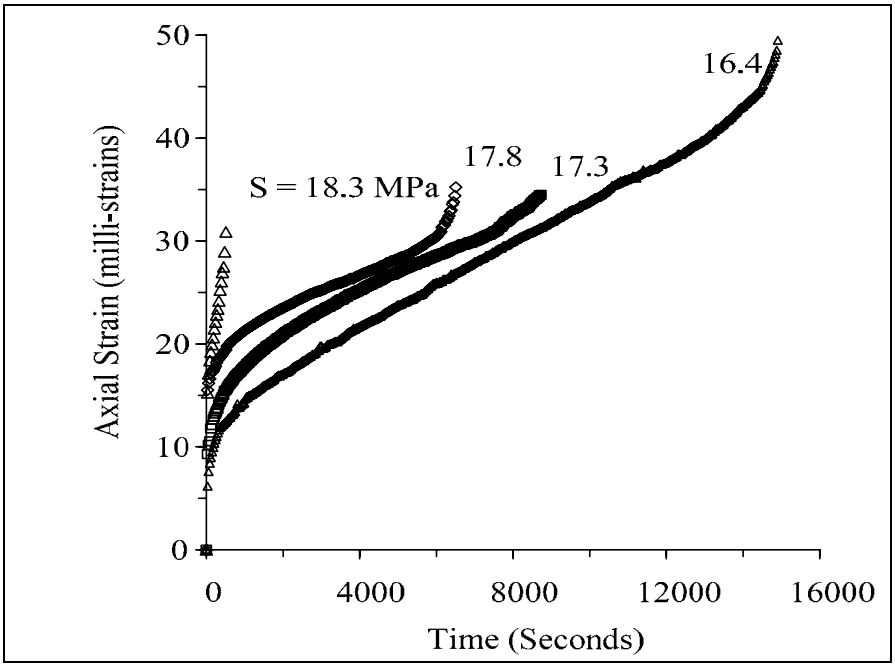

Figure 4.7 Axial strain–time curves from uniaxial cyclic loading tests.

4.3 Cyclic modified point load tests

4.3.1 Test Method

The objective of this test is to determine the true elastic modulus of the salt under MPL loading configurations. The cyclic MPL test is similar to uniaxial cyclic loading test. The point loading platens apply the axial loads to the circular disk specimens. The MPL tests are performed on salt specimens with thickness-to-loading point diameter ratio (t/d) of 2 and diameter of specimen-to-loading point diameter ratios (D/d) of 2 and 4. The MPL loading points (Figure 4.8) used in this study is 25 mm in diameter. The SBEL PLT-75 is used to test machine. The test apparatus is similar to that of the conventional point load (CPL) test (Figure 4.9), except the loading points are cut flat to have a circular cross-sectional area instead of half-spherical shape loading points (Tepnarong, P., 2001). Figure 4.10 shows examples of post-test specimens from the cyclic MPL tests. The loading frequency is 0.3 Hz. The maximum axial loads in each cycle are in range of 60% to 100% of the strength value and the minimum axial stress is maintained constant at 0.1 MPa for all specimens. The vertical deformations (δ) are monitored. A total of ten specimens have been tested.

4.3.2 Test Results

Results of cyclic MPL tests are shown in Table 4.3. The maximum axial stresses vary from 16 MPa to 24 MPa for D/d = 2 and 26 MPa to 34 MPa for D/d = 4 (about 60% to 100% of the compressive strength value). The strength value is determined by the compressive strength test (Figure 4.11). The MPL strength (P_{mpl}) is calculated by:

$$P_{mpl} = p_f / (\pi d^2 / 4) \text{ MPa} \qquad (4.3)$$

where p_f is the applied load at failure and d is the diameter of loading point. Figures 4.12 and 4.13 show the results of cyclic MPL test.

4.3.3 Discussions

The example of post-test specimens show the mode of failure in (Figure 4.14) shear cone which is usually formed underneath the loading points. Two or three tension-induced cracks are commonly found across the specimens.

The elastic modulus can be predicted by finite difference (FLAC) simulations. The simulation is made in axis-symmetric, assuming that the material is homogeneous and isotropic. Due to the presence of two symmetry planes (horizontal and vertical) across a center of specimen, only one quarter of the specimen has been modeled (Figure 4.15). The finite difference mesh and boundary conditions are designed for studying the effects of specimen diameter. The ratio of t/d is 2 and D/d varies from 1 to 8. The initially elastic modulus is assumed varies from 10 to 40 GPa. The series of finite difference (FLAC) simulations are shown in Figure 4.16. Results from the series of the simulations (Figure 4.17) yield a linear relation between the normalized stress applied under the MPL loading platen (ΔP) by the induced axial deformation ($\Delta\delta$) and the elastic modulus E as:

$$\Delta P/\Delta\delta = \alpha.E+\beta \qquad (4.4)$$

where α and β are empirical constants, depending on the specimen-to-platen diameter ratio (D/d). Using the test data from the cyclic MPL testing, the salt elastic modulus determined from this equation is calculated. Table 4.4 shows the results of elastic modulus calculation from cyclic MPL tests. The results of calculated elastic modulus value for D/d = 2 is 15.9±6.4 GPa, and for D/d = 4 is 14.9±4.0 GPa. Results of elastic

modulus values predicted from cyclic MPL tests are close to those obtained from uniaxial cyclic loading tests. Figure 4.18 shows the elastic modulus values calculated from the series of unloading curves as a function of loading cycles. The salt elasticity exponentially decreases as the number of loading cycle increases.

The failure (fatigue) stress decreases as the number of loading cycle (N) increases (Figure 4.19), which can be represented by the power equations, for D/d = 2 (Equation 4.3) and for D/d = 4 (Equation 4.4):

$$S = 23.92\ N^{(-0.053)}\ \text{MPa} \tag{4.5}$$

$$S = 34.61\ N^{(-0.035)}\ \text{MPa} \tag{4.6}$$

where S is maximum stress and N is number of loading cycle. Figure 4.20 shows the axial strain–time curves compiled from the unloading cycles. The curves show the transient, steady-state and tertiary creep phases which are similar to those obtained from the static creep testing.

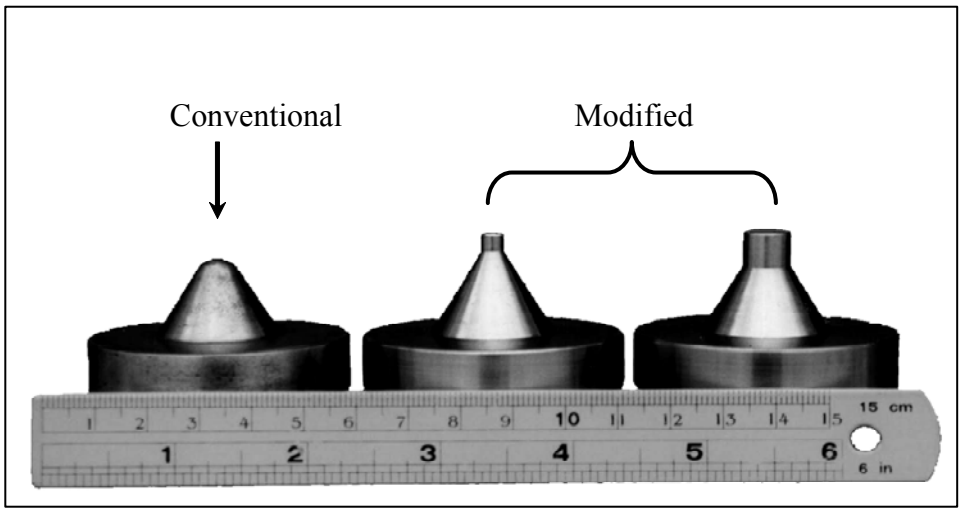

Figure 4.8 CPL and MPL loading points (from Tepnarong, P., 2001).

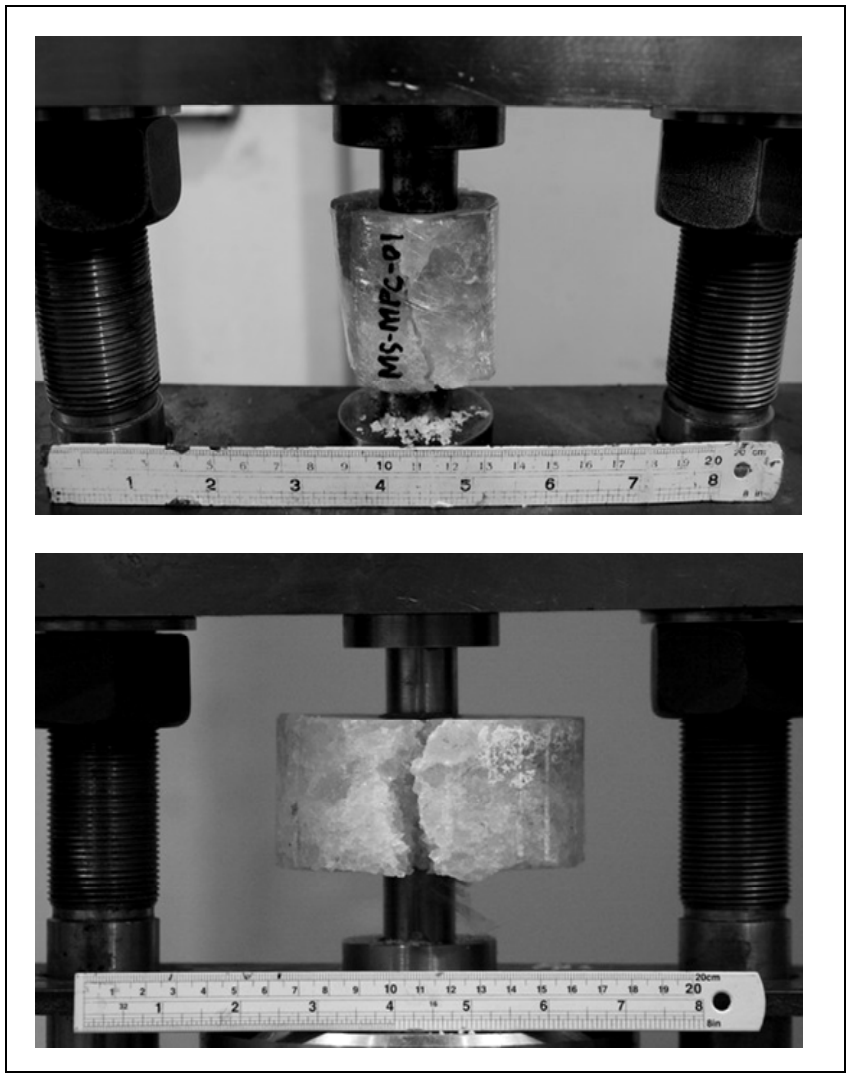

Figure 4.9 Examples salt specimens failed in testing machine for MPL cyclic loading test with D/d = 2 (top) and D/d = 4 (bottom).

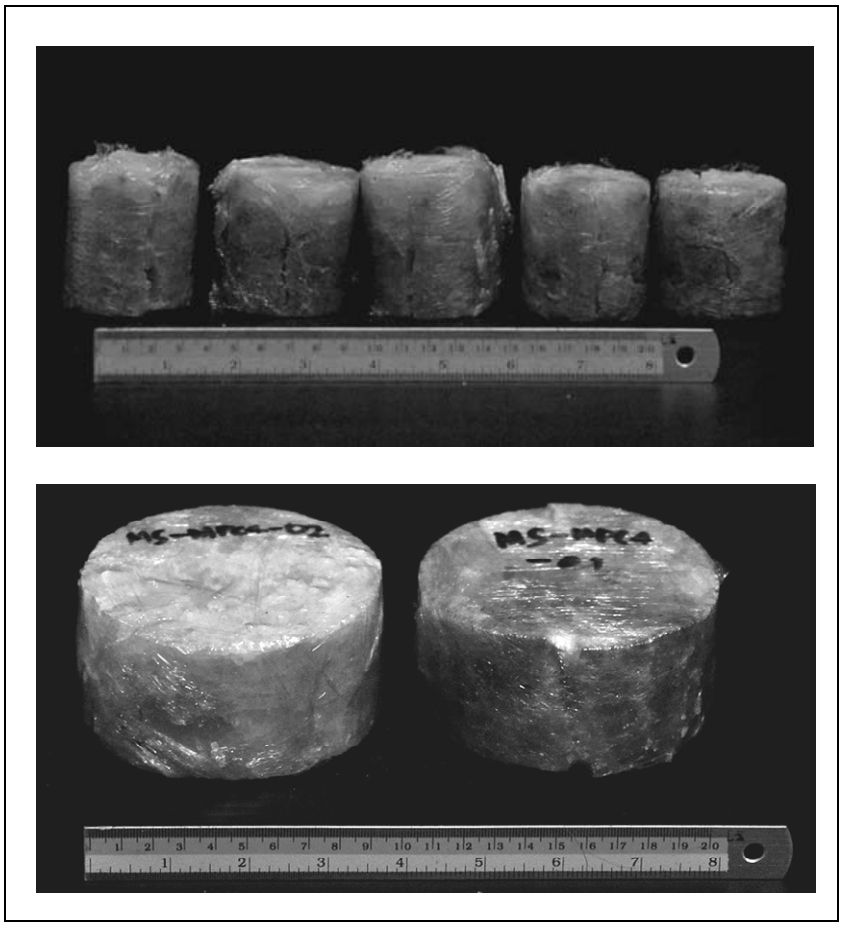

Figure 4.10 Examples of post-test specimens from the cyclic MPL test with D/d = 2 (top) and D/d = 4 (bottom).

Table 4.3 Results of cyclic MPL tests.

Specimen No.	D/d	Depth (m)	Density (g/cc)	Maximum Stress, P_{mpl} (MPa)	Number of Cycles
MS-MPC2-01	2	365.31-365.40	2.16	24	1
MS-MPC2-02		365.44-365.50	2.15	22	3
MS-MPC2-03		365.21-365.30	2.14	18	428
MS-MPC2-04		366.20-366.33	2.15	16	558
MS-MPC2-05		366.35-366.44	2.14	20	79
MS-MPC4-01	4	220.05-220.20	2.14	34	1
MS-MPC4-02		220.23-220.29	2.15	32	20
MS-MPC4-03		222.25-222.42	2.16	30	328
MS-MPC4-04		222.51-222.63	2.15	28	526
MS-MPC4-05		224.15-224.24	2.15	26	548

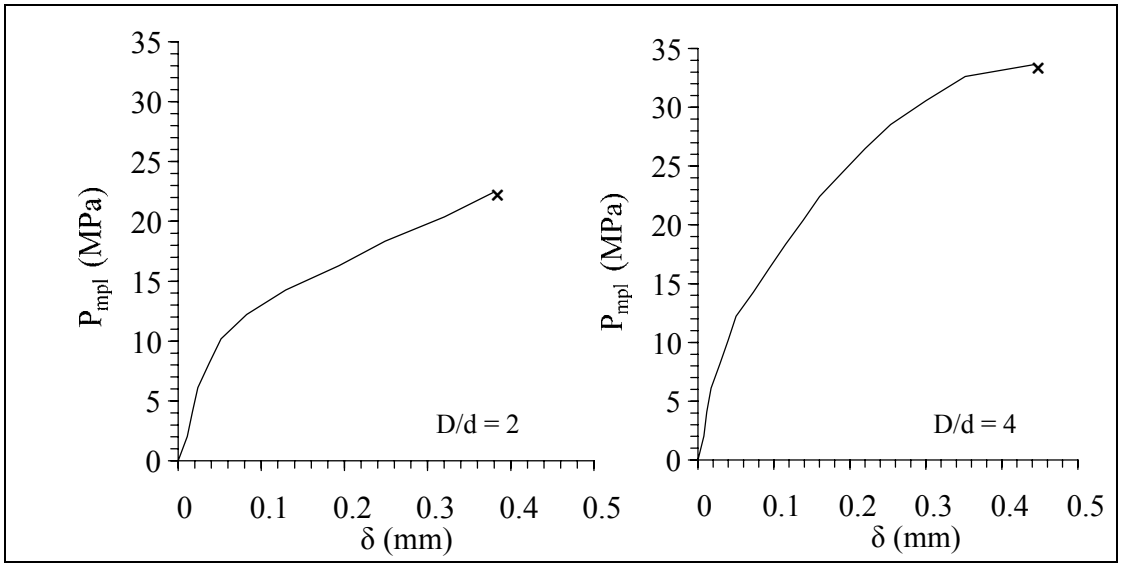

Figure 4.11 Result of compressive strength test for determine the strength value of cyclic MPL test with D/d = 2 (left) and D/d = 4 (right).

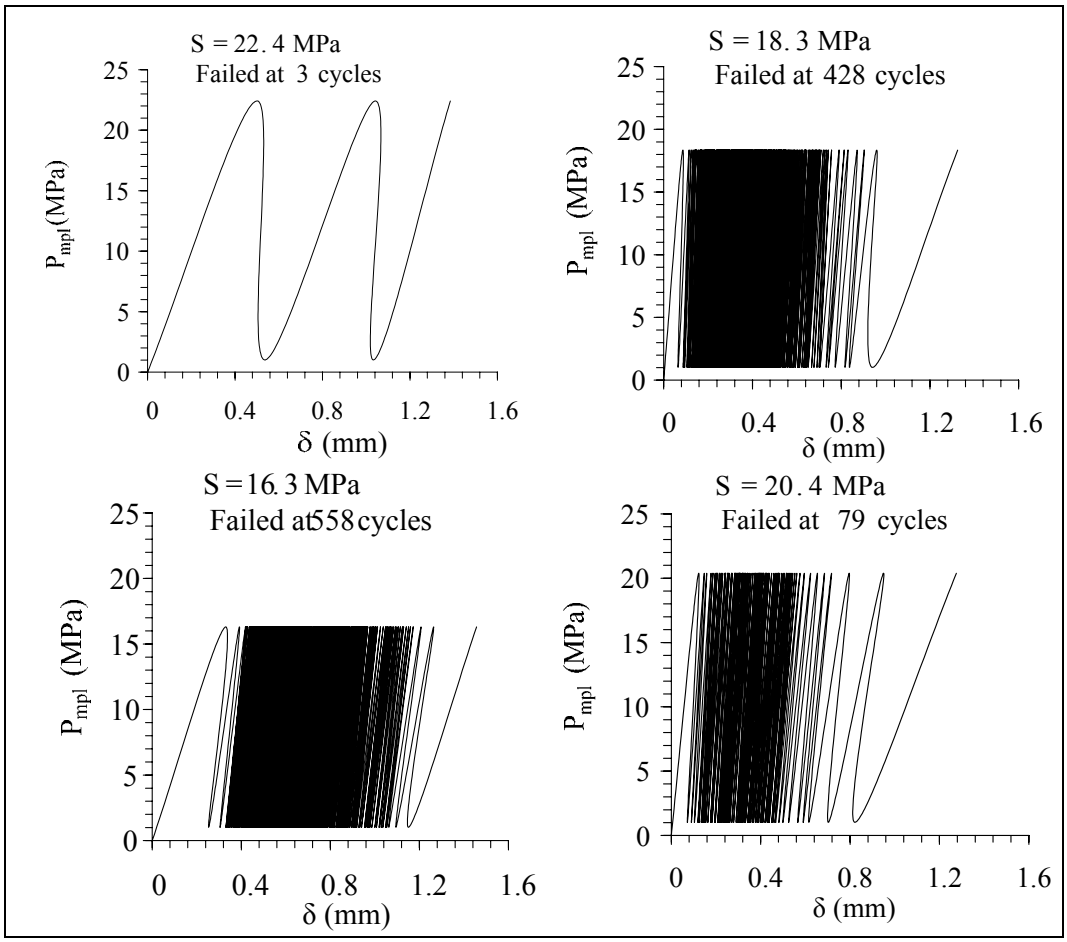

Figure 4.12 Results of cyclic MPL test results (D/d = 2). Axial stress (P_{mpl}) plotted as a function of axial displacement (δ).

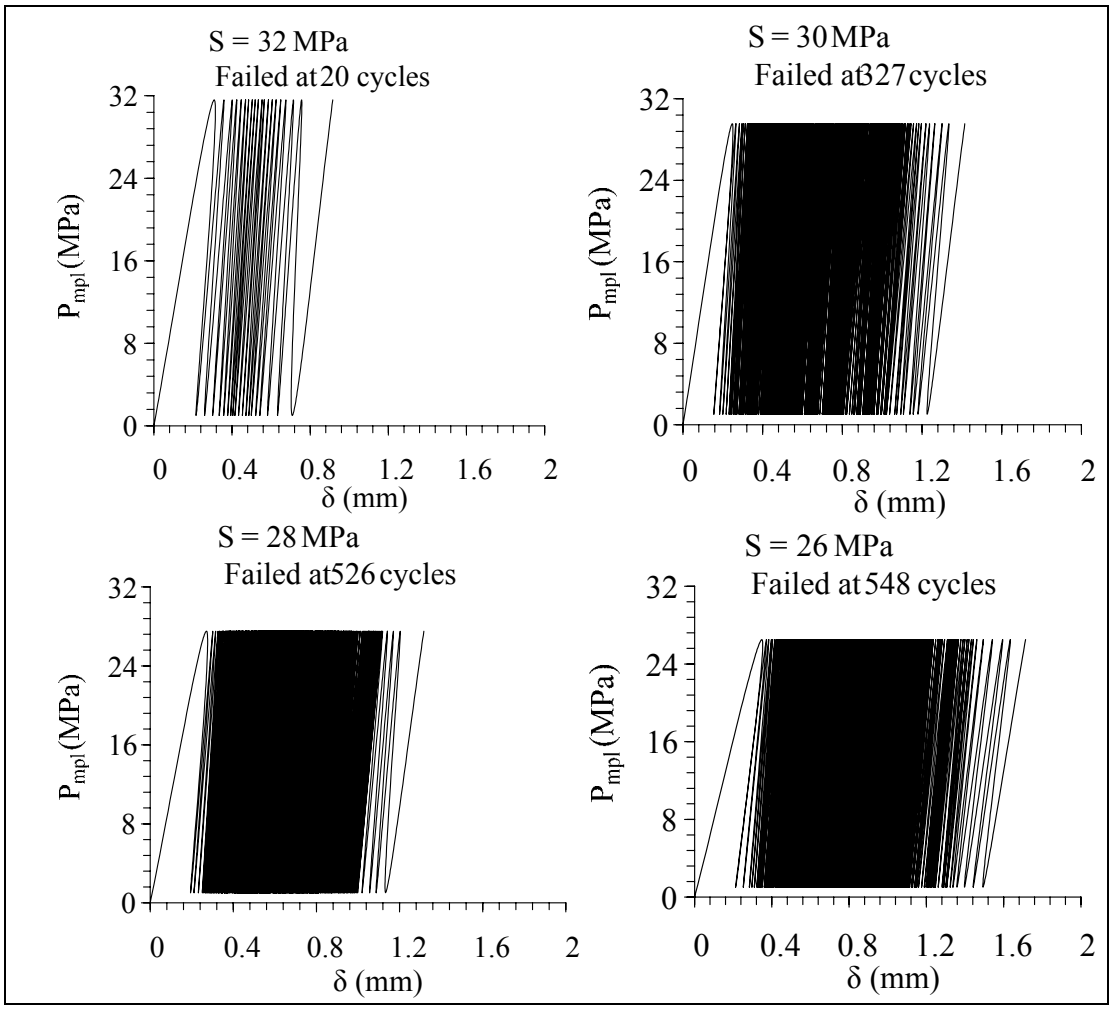

Figure 4.13 Results of cyclic MPL test results (D/d = 4). Axial stress (P_{mpl}) plotted as a function of axial displacement (δ).

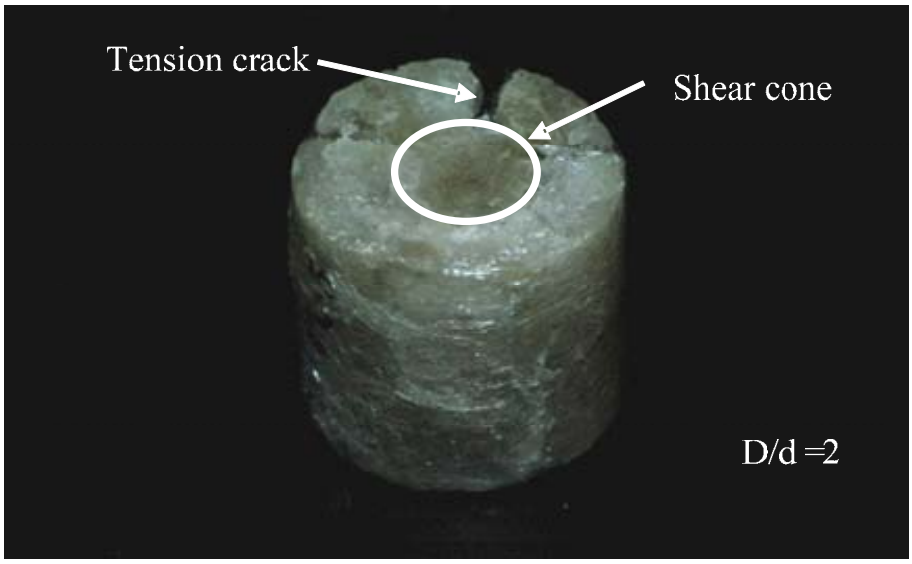

Figure 4.14 Post-test specimen, the tension-induced crack commonly found across the specimen and shear cone usually formed underneath the loading platens.

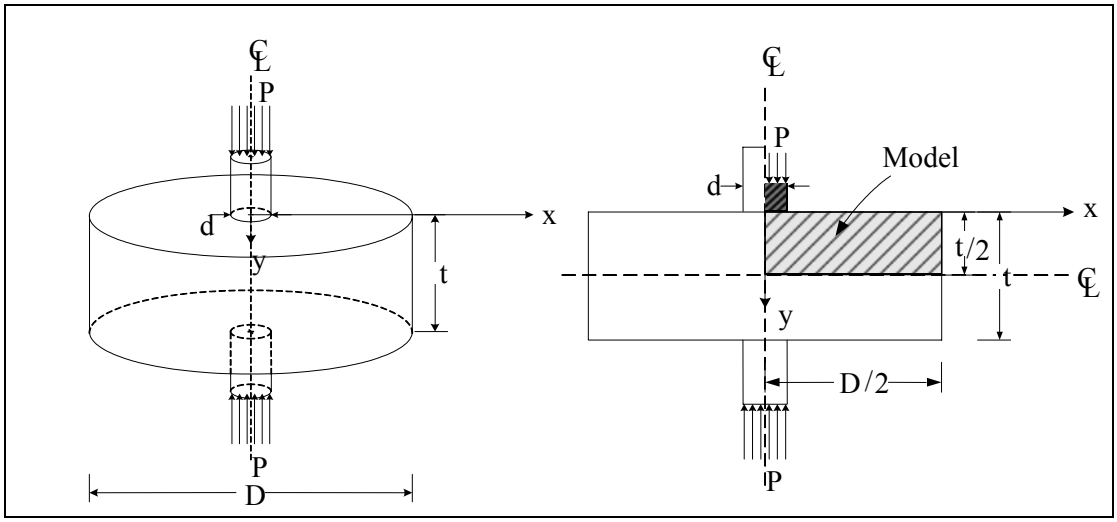

Figure 4.15 Boundary and loading conditions of model used to determine the elastic and creep parameters.

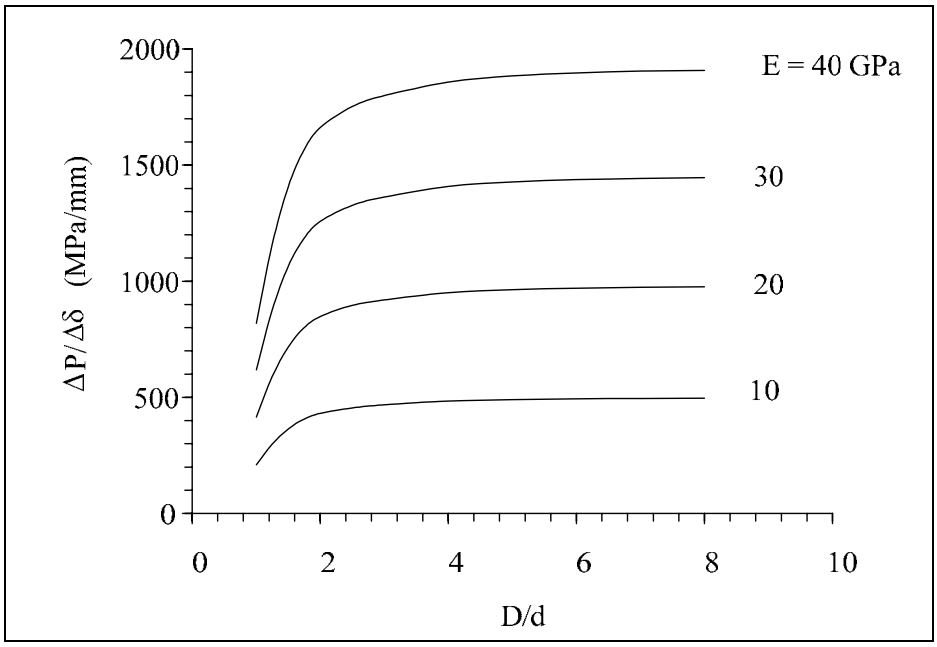

Figure 4.16 Series of finite difference (FLAC) simulations.

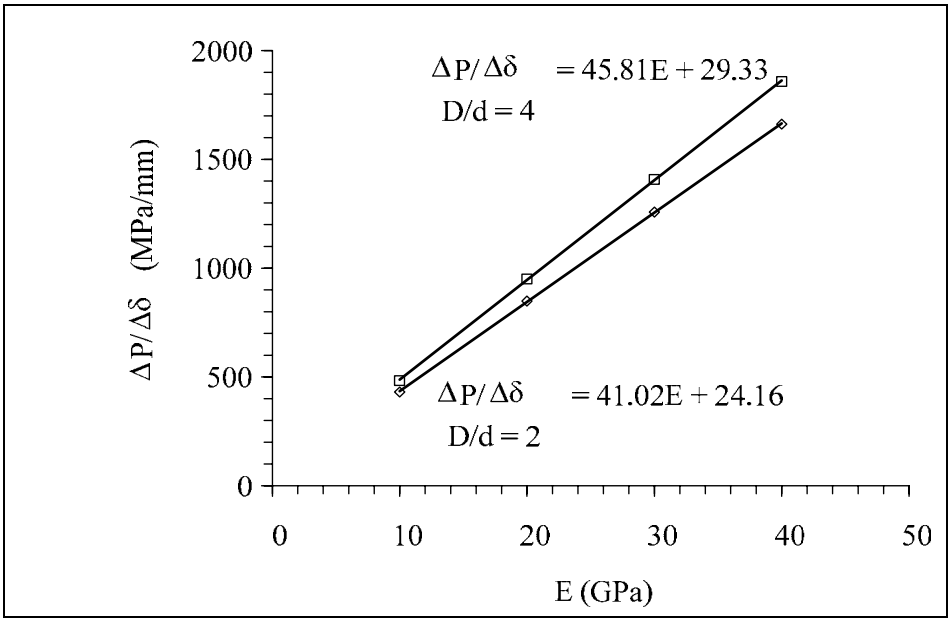

Figure 4.17 Results of FLAC simulations for predicting the elastic modulus from MPL testing.

Table 4.4 Results of elastic modulus calculation from cyclic MPL tests.

Specimen No.	D/d	Depth (m)	Density (g/cc)	Maximum Stress, P_{mpl} (MPa)	Number of Cycles	Elastic Modulus (GPa)
MS-MPC2-01	2	365.31-365.40	2.16	24	1	23.0
MS-MPC2-02		365.44-365.50	2.15	22	3	22.5
MS-MPC2-03		365.21-365.30	2.14	18	428	13.5
MS-MPC2-04		366.20-366.33	2.15	16	558	10.4
MS-MPC2-05		366.35-366.44	2.14	20	79	10.0
Mean±S.D.						15.9±6.4
MS-MPC4-01	4	220.05-220.20	2.14	34	1	21.1
MS-MPC4-02		220.23-220.29	2.15	32	20	16.5
MS-MPC4-03		222.25-222.42	2.16	30	328	13.0
MS-MPC4-04		222.51-222.63	2.15	28	526	12.5
MS-MPC4-05		224.15-224.24	2.15	26	548	11.3
Mean±S.D.						14.9±4.0

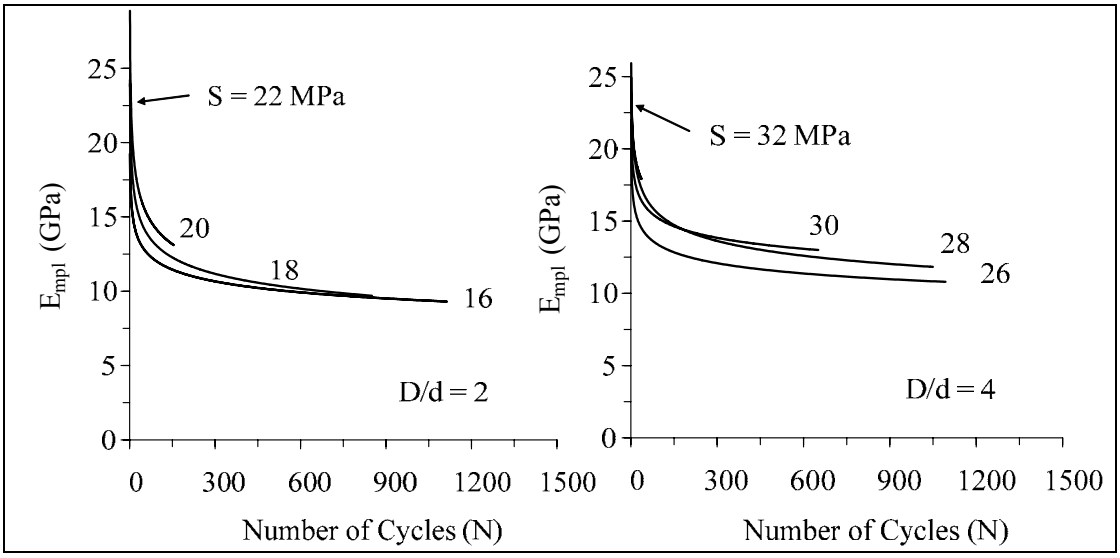

Figure 4.18 Elastic modulus plotted as a function of number loading cycles (N) up to failure with D/d = 2 (left) and 4 (right).

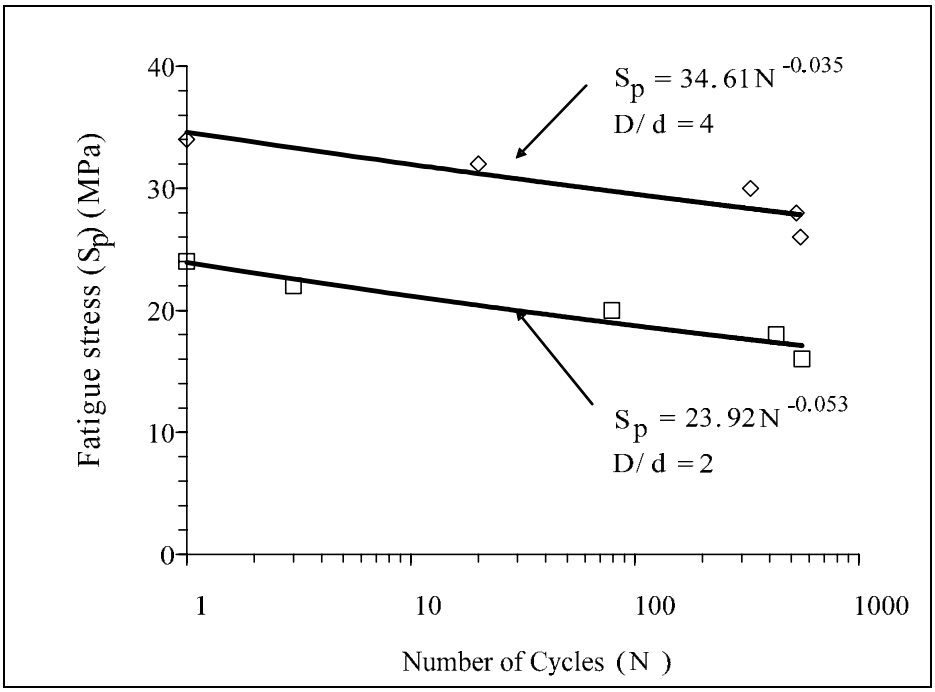

Figure 4.19 Failure stress (S_p) plotted as a function of number of point loading cycles at failure (N). D indicates the diameter of salt specimens.

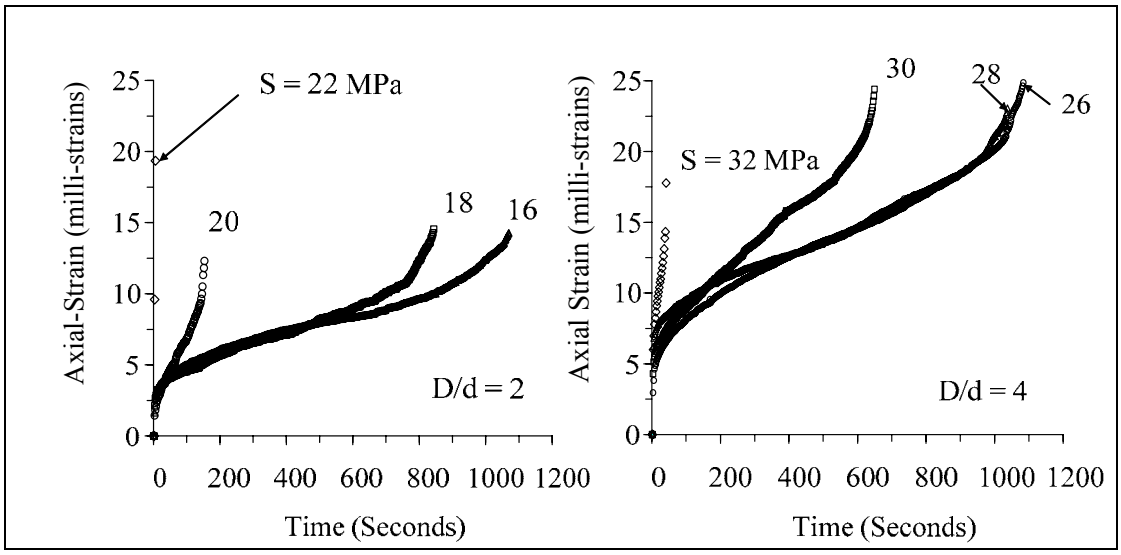

Figure 4.20 Axial strain–time curves from cyclic MPL tests with D/d = 2 (left) and D/d = 4 (right).

4.4 Triaxial creep tests

4.4.1 Test Method

The objective of triaxial creep tests is to determine the visco-plastic and visco-elastic parameters of the salt specimens under confined condition. The diameter of salt specimen is 54 mm (L/D = 2.0). Five specimens are tested under constant axial stresses from 31 to 50 MPa. The constant confining pressures are between 3 to 10 MPa and octahedral shear stress varies from 11.3 to 21.2 for a period of about 21 days. The experimental procedure follows the ASTM standard (ASTM D4406-93). A compression machine (Consolidation machine, capacity of 5,000 kN) is used to apply constant axial load onto the specimens. The salt specimens are placed into a triaxial (Hoek) cell to provide constant confining pressure (Figure 4.21). During the test, the axial deformation and time are recorded.

4.4.2 Test Results

The triaxial creep test is to determine time dependent behavior and to compare the creep deformation of salt specimens obtained from MPL creep tests. Figure 4.22 shows the post-tests specimen of triaxial creep tests. Table 4.5 illustrates summary results of the triaxial creep test. Results of triaxial creep tests are presented in forms of strain-time curves given in Figure 4.23. The curve represents transient steady state and tertiary state creep of salt specimens under a constant axial load and confining pressure.

4.4.3 Discussions

The instantaneous creep strain depends on the axial stress and confining pressure. In general the increase of the constant axial stress induces a larger

axial strain. The strain rate under higher axial stresses is greater than the one under lower axial stresses. The post-tested specimens show a small creep deformation. Some salt specimens show the micro-cracks extending along crystalline boundaries. The difference between the original diameters and the final diameter of the salt specimens is between 1 and 3%.

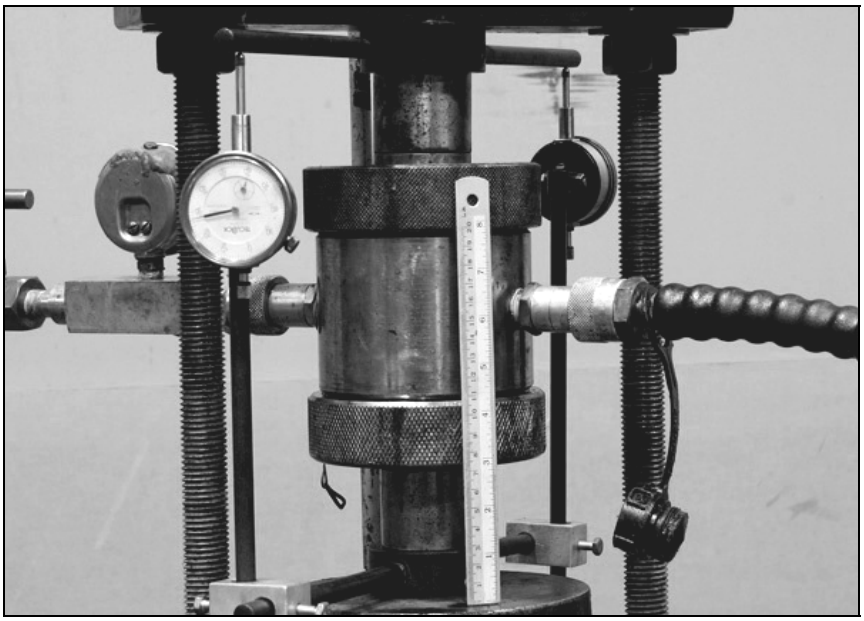

Figure 4.21 Salt specimens are placed into a triaxial (Hoek) cell.

Figure 4.22 Some specimen post-test of triaxial creep tests.

Table 4.5 Results of triaxial creep tests.

Specimen Number	Depth (m)	Density (g/cc)	Constant Axial Stress (MPa)	Confining Pressure (MPa)	Time (Days)
MS-TCR-01	250.21-250.42	2.17	39	3	55 min
MS-TCR-02	250.45-250.59	2.15	35	5	21
MS-TCR-03	252.36-252.54	2.17	40	10	21
MS-TCR-04	251.20-251.39	2.16	50	5	21
MS-TCR-05	255.67-256.02	2.17	31	7	21

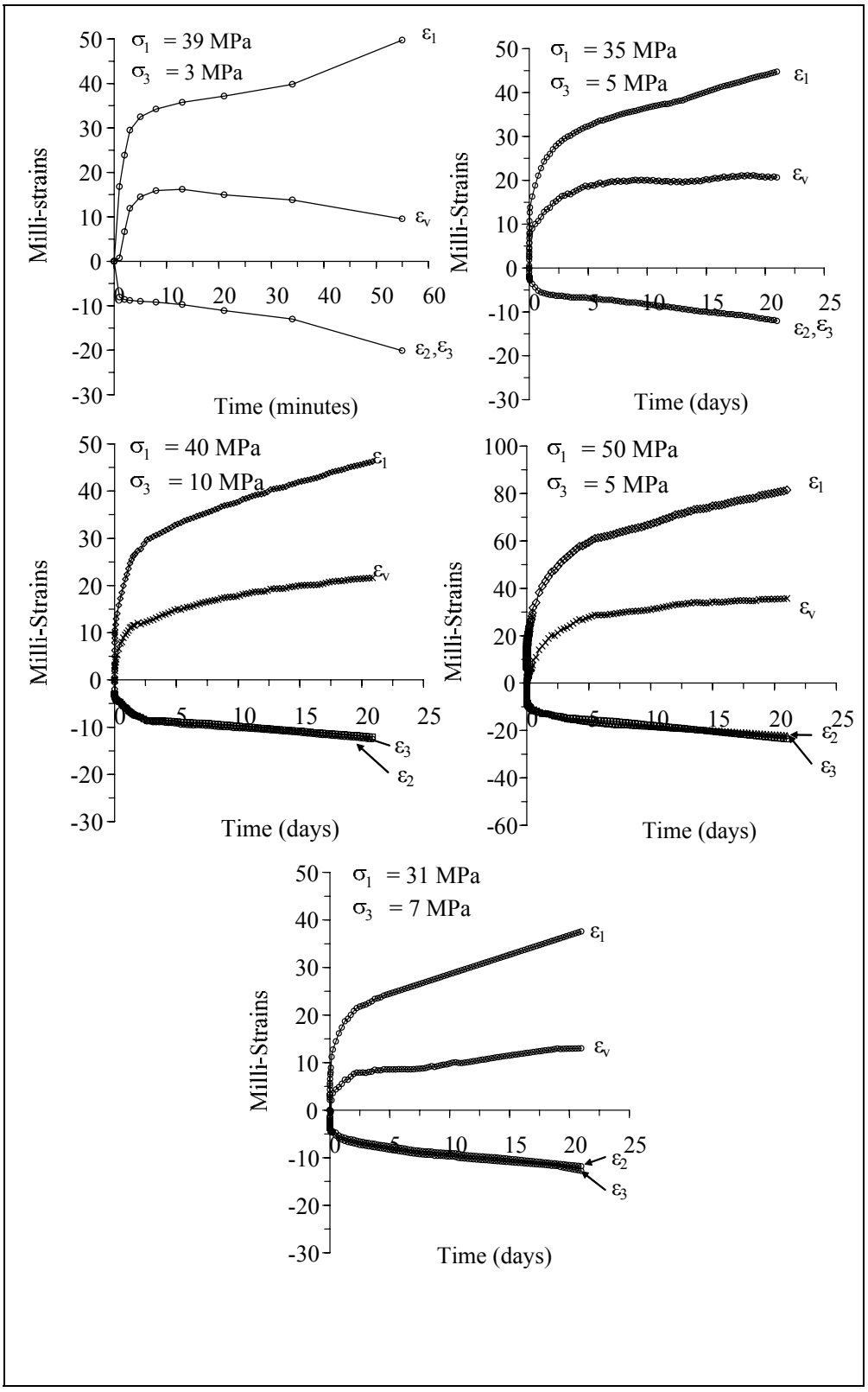

Figure 4.23 The strains-time curves from triaxial creep tests.

4.5 Modified point load creep testing

4.5.1 Test Method

The MPL creep tests have been performed to determine the time-dependent properties of the salt under isothermal condition. The test is similar to uniaxial creep test. The results will be used to calibrate the visco-plastic and visco-elastic parameters coefficient of the salt. The diameters of salt specimens are 48 mm and 101 mm. The MPL loading points used in this study is 25 mm in diameter. A compression machine (Consolidation machine, capacity of 5,000 kN) is used to apply constant axial load onto the specimens. The tests are performed on salt specimens with thickness-to-loading point diameter ratio (t/d) of 2, with diameter of specimen-to-loading point diameter ratio (D/d) of 2 and 4. The axial deformation (δ) is monitored for various applied axial stresses up to 30 days or until failure occurs. Some examples of specimen placed in loading machine during loading are given in Figure 4.24. The post-test specimens are shown in Figure 4.25. A total of ten specimens have been tested.

4.5.2 Test Results

The results of MPL creep tests are given in Table 4.6. For the MPL testing, the applied constant axial stresses (P_{mpl}) vary from 8 MPa to 16 MPa for D/d = 2 and 14 MPa to 25 MPa for D/d = 4. Figure 4.26 shows the results of the axial displacement plotted as a funtion of time. The curve represents transient steady state and tertiary state creep of salt specimens under a constant axial stresses.

4.5.3 Discussions

The post-test specimens show a small creep deformation. Post-test specimens failed show the modes of failure in (Figure 4.27) shear cone which is

usually formed underneath the loading points. Two or three tension-induced cracks are commonly found across the salt specimens. The instantaneous creep strain depends on the axial stress. Rate of the axial deformation under higher axial stresses is greater than the one under lower axial stresses.

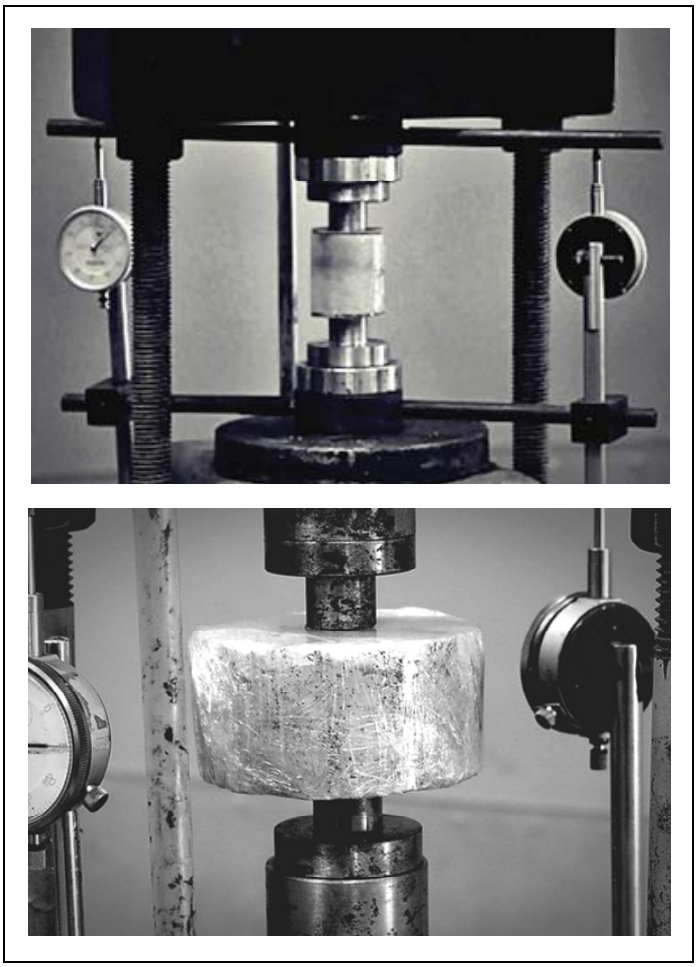

Figure 4.24 Somes salt specimens placed in a loading machine with D/d = 2 (top) and D/d = 4 (bottom).

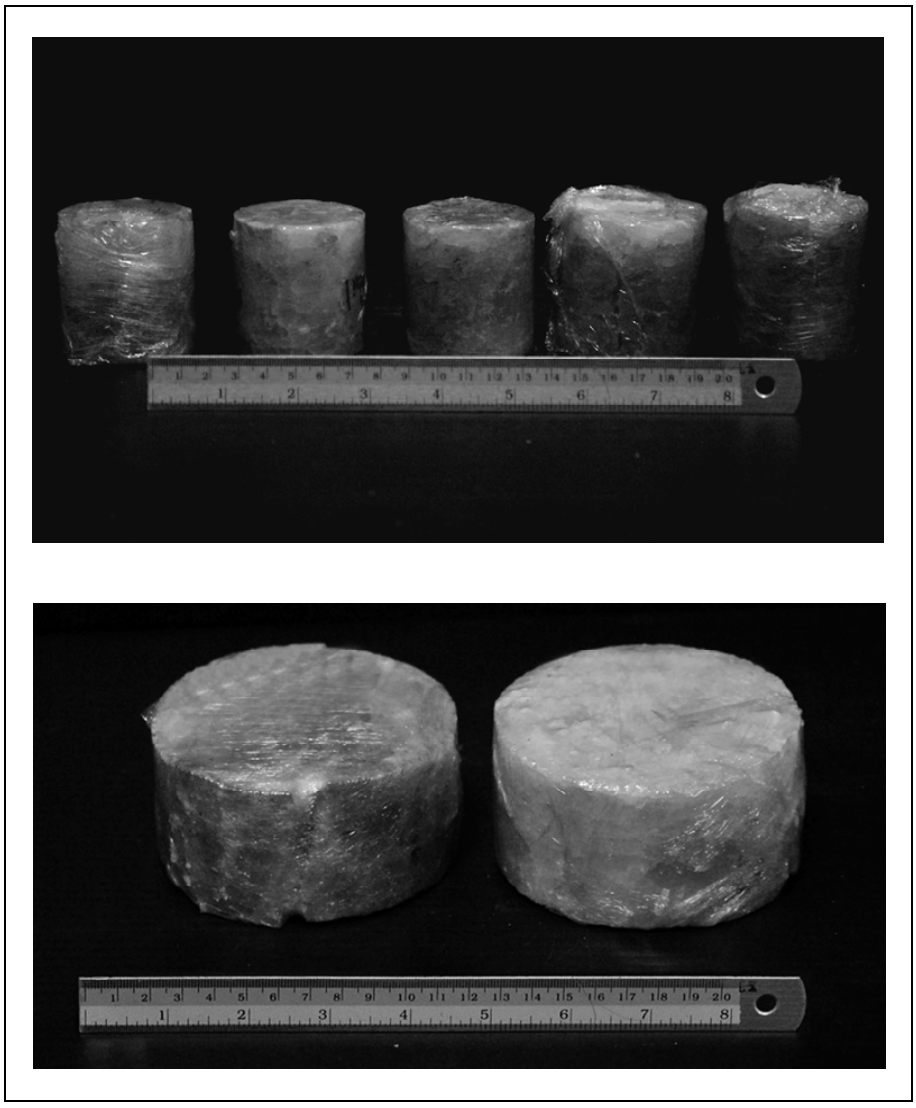

Figure 4.25 Some specimen post-test of MPL creep tests with D/d = 2 (top) and D/d = 4 (bottom).

Table 4.6 Results of MPL creep tests.

Specimen Number	D/d	Depth (m)	Density (g/cc)	Constant Axial Stress, P_{mpl} (MPa)	Time (Days)
MS-MCR2-01	2	345.15-345.28	2.16	16	12
MS-MCR2-02		346.21-346.29	2.15	14	14
MS-MCR2-03		345.35-345.40	2.21	12	30
MS-MCR2-04		346.42-346.51	2.17	10	30
MS-MCR2-05		346.55-346.64	2.16	8	30
MS-MCR4-01	4	208.15-209.23	2.15	25	6
MS-MCR4-02		209.45-209.54	2.17	24	30
MS-MCR4-03		209.61-209.70	2.19	20	30
MS-MCR4-04		208.05-208.12	2.15	18	30
MS-MCR4-05		211.37-211.52	2.16	14	30

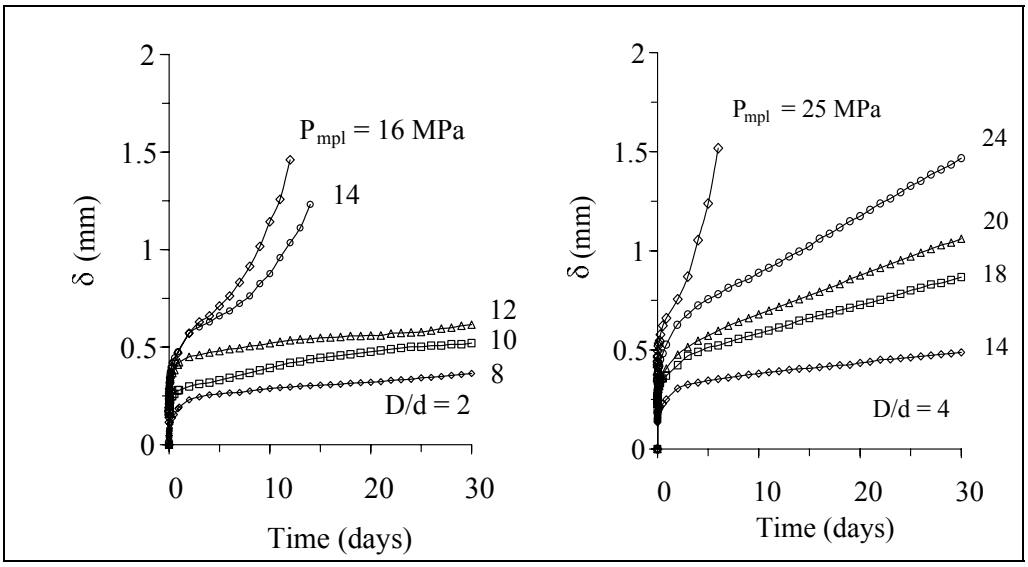

Figure 4.26 Results of the MPL creep tests with D/d = 2 (left) and D/d = 4 (right).

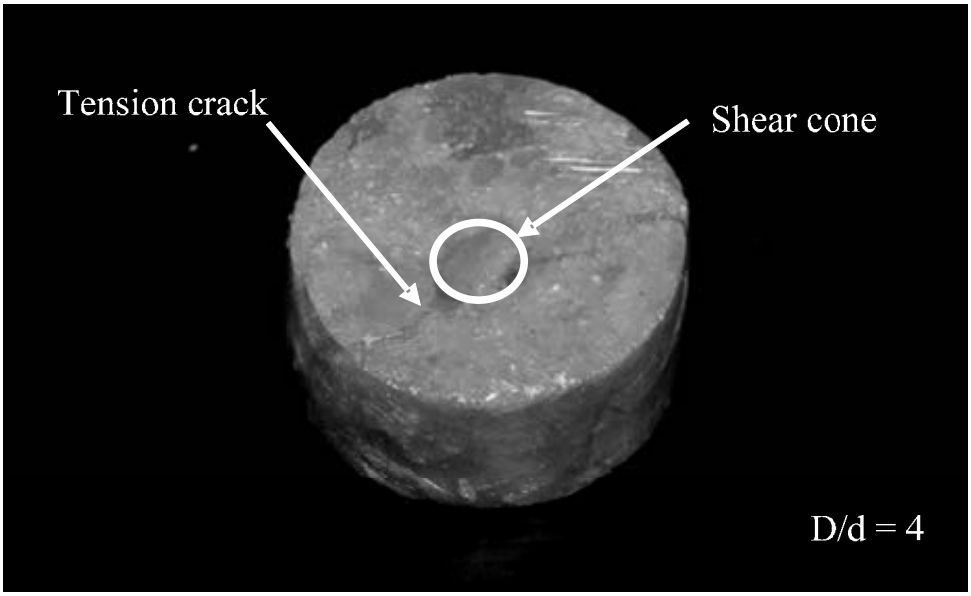

Figure 4.27 A post-test specimen, the tension-induced crack commonly found acrossthe specimen and shear cone usually formed underneath the loading platens.

CHAPTER V

SALT PROPERTIES CALIBRATION

5.1 Introduction

The purpose of this chapter is to describe the calibration of salt property parameters. The regression analysis on the linear visco-elastic equation of the Burgers model and the finite difference code (FLAC) is employed in the calibration. The data used in the calibration are obtained from the triaxial creep tests and MPL creep tests. These parameters include the elastic modulus, the viscoelastic and the viscoplastic coefficients. The elastic and time-dependent parameters from the MPL testing results are compared with those calibrated from the conventional triaxial methods to assess the reliability of the MPL creep testing.

5.2 Calibration from triaxial creep tests

The objective of the calibration is to determine the properties parameters of the salt specimens under confining pressures. The time-related parameters are monitored, recorded and analyzed. Results from the triaxial creep tests provide the data basis for the time-dependent properties on rock salt based on the conventional approach. The simple rheological creep models are used to describe behavior of the salt, i.e., Burgers model (Richards, 1993). The regression analysis is used to calibration. The relation between the octahedral shear stress (τ_{oct}) and octahedral shear strain (γ_{oct}) are determined. The octahedral shear strains (γ_{oct}) for the triaxial test conditions are plotted as a function of time. They are calculated by:

$$\gamma_{oct} = [((\varepsilon_1 - \varepsilon_2)^2 + (\varepsilon_1 - \varepsilon_3)^2 + (\varepsilon_2 - \varepsilon_3)^2) / 3]^{1/2} \quad (5.1)$$

where γ_{oct} is octahedral shear strain, ε_1 is the major principal strain, ε_2 is the intermediate principal strain, and ε_3 is the minor principal strain.

The linear elastic relation between octahedral shear strain and stress can be written as (Jaeger and Cook, 1979):

$$\gamma_{oct} = \tau_{oct} / 2G \quad (5.2)$$

where τ_{oct} is octahedral shear stress, G is shear modulus.

Using the Laplace transformation a linear visco-elastic relation can be derived from the above equation as follows (Jaeger and Cook, 1979):

$$\gamma_{oct}(t) = \tau_{oct}\left[\frac{E_2 t}{\eta_1\eta_2} - \frac{1}{\eta_1}(1-\exp(\frac{-E_2 t}{\eta_2})) + (\frac{E_2}{\eta_2 E_1} + \frac{1}{\eta_2} + \frac{1}{\eta_1})(1-\exp(\frac{-E_2 t}{\eta_2})) + \frac{1}{E_1}\exp(\frac{-E_2 t}{\eta_2})\right] \quad (5.3)$$

where γ_{oct} (t) is octahedral shear strain which is a function of time, t is time, E_1 is elastic modulus, E_2 and η_2 are visco-elastic parameters and η_1 is visco-plastic parameter. Table 5.1 shows the creep property parameters calibrated from the triaxial creep tests. Figure 5.1 shows the curves fitting between the calibration and the experimental results for the triaxial creep test.

Table 5.1 Creep property parameters calibrated from the triaxial creep tests.

Constant axial stress (MPa)	Confining pressure (MPa)	τ_{oct} (MPa)	E_1 (GPa)	E_2 (GPa)	η_1 (GPa.day)	η_2 (GPa.day)
31	7	11.3	2.0	1.20	20.0	1.38
35	5	14.1	1.9	0.98	19.0	1.35
39*	3	14.1	-	-	-	-
40	10	16.9	2.0	0.78	19.0	1.10
50	5	21.2	2.1	0.58	18.0	0.84
Mean±S.D.			2.00±0.08	0.89±0.27	19.0±0.82	1.17±0.30

Note: * is specimen failed

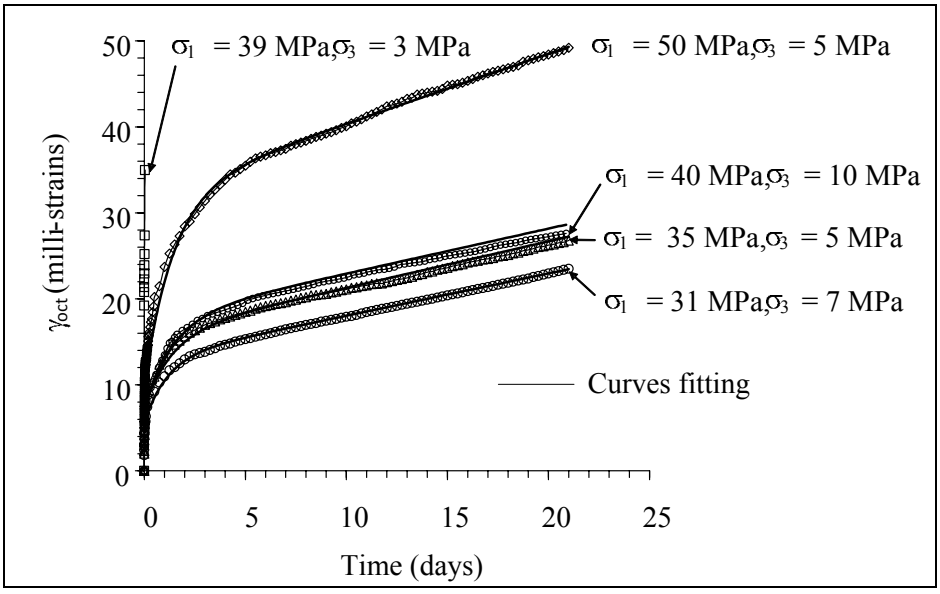

Figure 5.1 Results of calibrations for the triaxial creep tests. Octahedral shear strain (γ_{oct}) plotted as a function of time.

5.3 Calibration from MPL creep tests

To assess the effect of the time-dependent properties on salt for the MPL creep tests, the Burger model is used to calibrate with the test data. The salt property calibration of the MPL creep tests uses regression method and numerical simulations

(FLAC). These elastic and time-dependent parameters can be calibrated from the laboratory experiment results. Tepnarong (2006) proposed an empirical equation to correlate the elastic modulus of the MPL specimen with the ratio of the applied load-to-vertical deformation ratio as:

$$E_{mpl} = (\frac{t}{\alpha_E})(\frac{\Delta P}{\Delta \delta}) \tag{5.4}$$

where E_{mpl} is elastic modulus predicted by MPL test, α_E is displacement function obtained from numerical analysis, $\Delta P/\Delta \delta$ is the stress change to displacement ratio obtained from unloading curves, and t is the specimen thickness. The displacement function α_E (Tepnarong, 2006) can be defined as: $\alpha_E = 4.1$ for D/d = 2 and $\alpha_E = 4.6$ for D/d = 4. This elastic relation is used to develop a visco-elastic governing equation by assuming that the salt creep behavior follows the Burgers model (Richards, 1993). The corresponding visco-elastic relation based on the Burgers model can be derived as:

$$\Delta\delta(t) = \frac{L \cdot \Delta P}{\alpha_E}\left[\frac{1}{9K} + \frac{2}{3}\left[\frac{t}{\eta_1} + \left(\frac{1}{E_2} + \frac{(\eta_2 - 1)}{\eta_1 E_2} + \frac{(1+\eta_2)}{E_1}\right)\left(1 - \exp(\frac{-E_2 t}{\eta_2})\right)\right]\right] \tag{5.5}$$

where $\Delta\delta(t)$ is displacement which is a function of time, L is the specimen length (thickness), K is bulk modulus, E_1 is elastic modulus, E_2 and η_2 are visco-elastic parameters and η_1 is visco-plastic parameter.

Series of numerical simulations (FLAC) are also performed to calibrate the results from the MPL creep tests. This is made in axis-symmetric, assuming that the material is homogeneous and isotropic. Due to the presence of two symmetry planes

(horizontal and vertical) across a center of specimen, only one quarter of the specimen has been modeled. The models of salt specimen used in the calibration of properties parameters are given in Figure 5.2. The salt properties are assumed that the salt creep behavior follows the Burgers model. Tables 5.3 and 5.4 summarize the creep property parameters calibrated from the MPL creep tests. Figure 5.3 shows the comparison between the calibrations of experimental results, regression analysis and numerical simulations (FLAC).

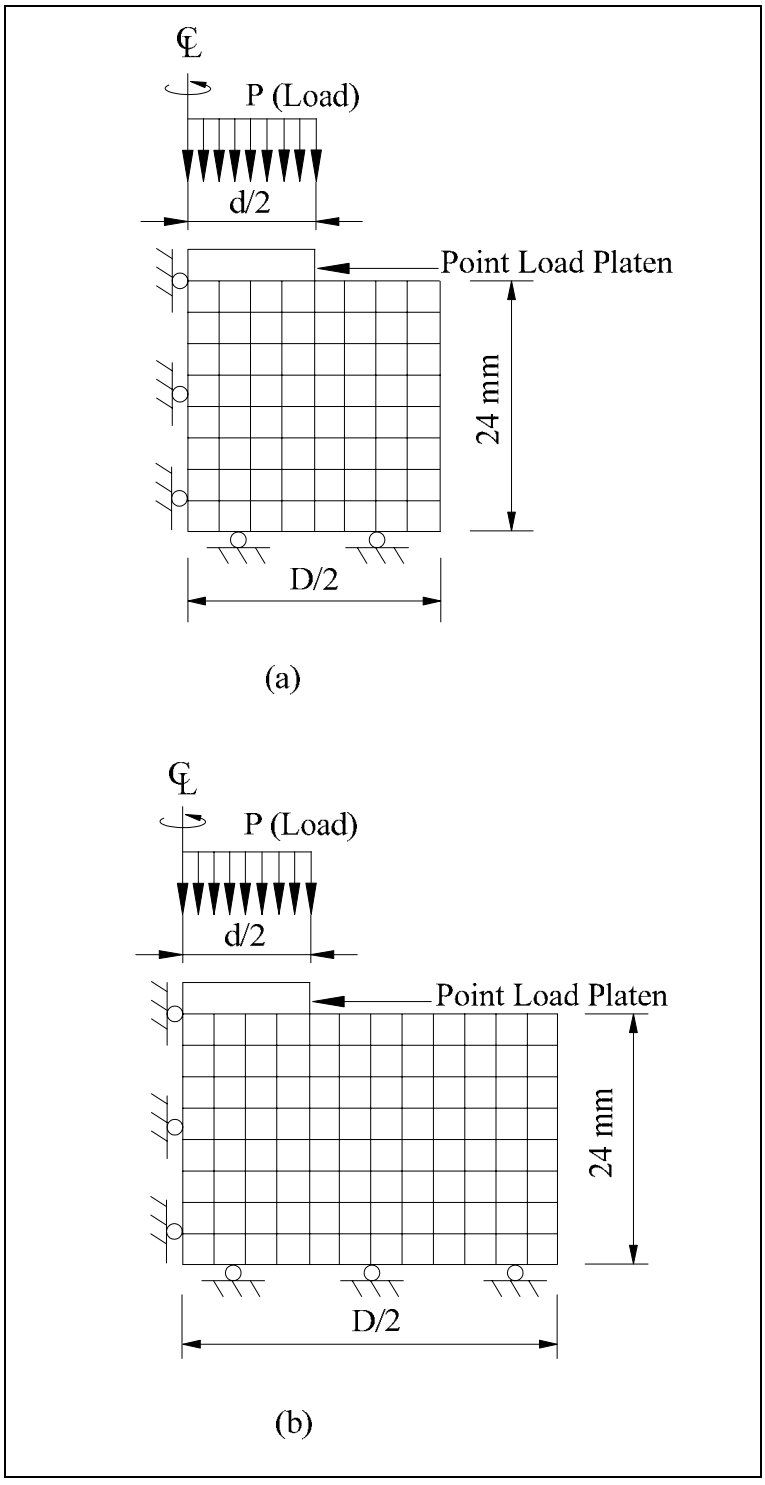

Figure 5.2 FLAC models of salt specimen used in the simulations and calibration of properties parameters, (a) D/d = 2, and (b) D/d = 4.

Table 5.2 Creep properties parameters calibrated from MPL creep tests with D/d = 2.

Test Method	Axial stress (MPa)	E_1 (GPa)	E_2 (GPa)	η_1 (GPa.day)	η_2 (GPa.day)
MPL creep test (D/d = 2)	8	1.80	1.30	16.00	1.10
	10	1.80	1.30	11.00	1.00
	12	1.90	1.30	11.00	1.00
	14	1.80	1.20	4.50	0.80
	16	1.80	1.00	2.50	0.40
	Mean±S.D.	1.82±0.04	1.22±0.13	9.00±5.47	0.86±0.28
FLAC simulations (D/d = 2)	8	0.86	0.37	16.00	0.80
	10	0.86	0.27	14.90	0.76
	12	0.58	0.24	13.70	0.53
	14	0.58	0.20	3.00	0.40
	16	0.58	0.20	2.00	0.40
	Mean±S.D.	0.69±0.16	0.26±0.07	9.92±6.83	0.58±0.19

Table 5.3 Creep property parameters calibrated from MPL creep tests with D/d = 4.

Test Method	Axial stress (MPa)	E_1 (GPa)	E_2 (GPa)	η_1 (GPa.day)	η_2 (GPa.day)
MPL creep test (D/d = 4)	14	2.00	1.10	19.00	1.20
	18	1.90	1.10	9.00	0.80
	20	2.00	1.00	7.00	0.60
	24	1.90	1.00	5.60	0.60
	25	1.80	0.60	2.50	0.10
	Mean±S.D.	1.9±0.08	0.96±0.21	8.62±6.27	0.66±0.39
FLAC simulations (D/d = 4)	14	0.81	0.37	14.90	0.72
	18	0.75	0.37	11.90	0.72
	20	0.75	0.37	4.40	0.74
	24	0.84	0.37	2.80	0.60
	25	0.66	0.38	1.51	0.49
	Mean±S.D.	0.76±0.07	0.37±0.004	7.10±5.94	0.65±0.11

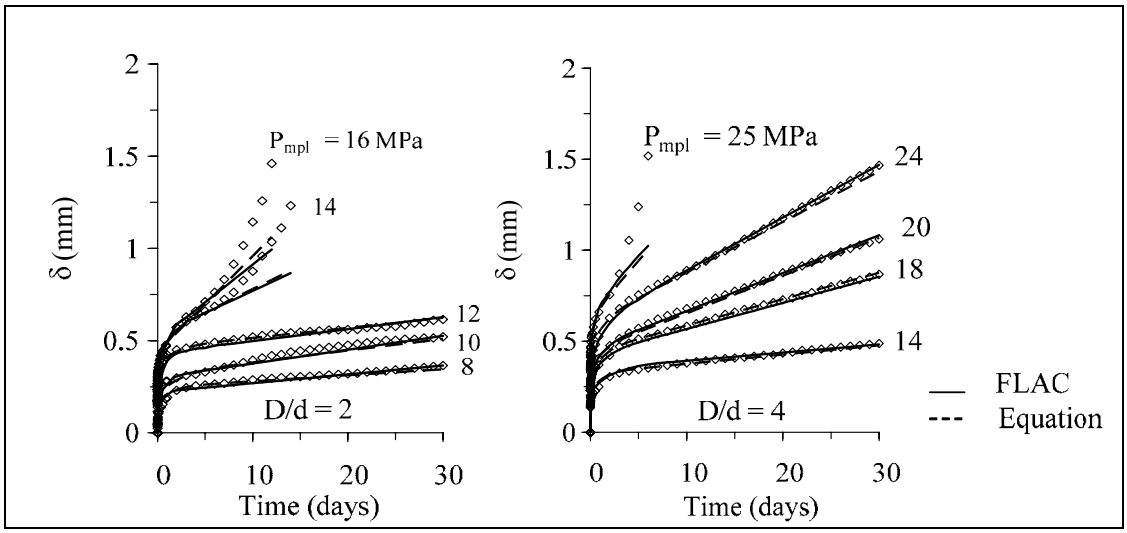

Figure 5.3 Results of calibrations for MPL creep tests with D/d = 2 (left) and 4 (right).

5.4 Discussions

The time-dependent parameters from the MPL testing results are compared with those calibrated from the conventional creep methods. The time-dependent parameters for different tests are compared in Table 5.4. The elastic parameters (E_1, E_2) obtained from the MPL creep testing is closer to those from the triaxial creep testing and the value from numerical simulation (FLAC) is the smallest. The viscosity coefficients (η_1 and η_2) from the conventional triaxial creep testing are about 50% greater than those from the MPL testing. Most of parameters calibrated from the numerical simulation (FLAC) tend to be less than those calibrated from the conventional triaxial creep testing and the MPL creep testing. Some discrepancies are probably due to scale effects on the MPL results and the intrinsic variability among the salt specimens. The MPL testing specimens are subjected to a stress gradient and

to a low value of the minimum principal stress while the conventional triaxial creep test specimens are subjected to uniform compressive stresses.

Table 5.4 Comparisons of the creep properties from different tests.

Test Methods	**E_1 (GPa)**	**E_2 (GPa)**	**η_1 (GPa.day)**	**η_2 (GPa.day)**
MPL Creep Test (D/d = 2)	1.82±0.04	1.22±0.13	9.00±5.47	0.86±0.28
FLAC simulation (D/d = 2)	0.69±0.16	0.26±0.07	9.92±6.83	0.58±0.19
MPL Creep Test (D/d = 4)	1.90±0.08	0.96±0.21	8.62±6.27	0.66±0.39
FLAC simulation (D/d = 4)	0.76±0.07	0.37±0.004	7.10±5.94	0.65±0.11
Triaxial Creep Test	2.00±0.08	0.89±0.27	19.0±0.82	1.17±0.30

CHAPTER VI

DISCUSSIONS, CONCLUSIONS AND RECOMMENDATIONS FOR FUTURE STUDIES

6.1 Discussions and conclusions

The objective of this research is to determine the time-dependent properties of rock salt using the MPL testing technique. This technique is proposed here as an alternative method of determining the time-dependent properties of creeping rocks in the laboratory. This thesis describes the detailed test methods, the derivation of the visco-elastic governing equation, and the predictive capability of the proposed MPL creep testing technique.

The elastic modulus obtained from the MPL testing can be predicted by finite difference (FLAC) simulations. The simulation is made in axis-symmetry. Results from the series of the simulations yield a linear relation between the normalized stress applied under the MPL loading platen (ΔP) by the induced axial deformation ($\Delta\delta$). The elastic modulus values obtained from the cyclic MPL tests loading are similar to those obtained from the uniaxial cyclic loading tests. The agreement also confirms that the proposed elastic relation is adequate to correlate the applied axial stress with the axial deformation for the MPL specimen and to relate them with the specimen elastic modulus.

The regression in performed on the linear visco-elastic equation of the Burgers model and the finite difference code (FLAC) employed in the calibration. The data

used in the calibration are obtained from the triaxial creep tests and MPL creep tests. These parameters include the elastic, the viscoelastic and the viscoplastic parameters. The elastic parameters (E_1, E_2) obtained from the MPL creep testing is closer to those from the triaxial creep testing. Some discrepancies are probably due to scale effects on the MPL results and the intrinsic variability among the salt specimens. The viscosity coefficients (η_1 and η_2) from the MPL testing are about 50% less than those from the conventional triaxial creep testing. This is probably because the load-displacement relation (Eqn. (5.4)) proposed by Tepnarong, P. (2006) may not truly represent the actual behavior of the salt under MPL test condition. Due to the simplicity of the MPL test procedure (compared to the triaxial creep test method) the MPL creep testing may become preferable method to determine the creep parameters of the salt under triaxial condition. The MPL results tend to be more conservative than those of the conventional method, i.e. yielding the lower values of viscosity coefficients. It should be noted that no intention is made here to replace the standard test methods of determining the time-dependent properties of the creeping rocks (i.e. ASTM). The proposed MPL testing technique can be useful for the cases where a standard core length (L/D ratio of 2.0-3.0) can not be obtained from the soft or fractured rocks.

6.2 Recommendations

The assessment of predictive capability of the proposed MPL testing technique has been limited to rock salt. Verification of the MPL proposed concept should be tested under a wider range of rock types. More testing is needed to confirm the applicability and limitations of the proposed, such as true triaxial creep test, multi-step triaxial loading, and triaxial cyclic loading test. The effects of loading rate and effect

of temperature should be considered. The constitutive law used in this study may not be adequately describe the salt behavior. Other constitutive laws, such as power laws and structural laws may be needed to describe the salt behavior.

REFERENCES

ASTM D4543-08. Standard practice for preparing rock core specimens and determining dimensional and shape tolerances. **Annual Book of ASTM Standards**, Vol. 04.08. West Conshohocken, PA: ASTM.

ASTM D2664-95a. Standard test method for triaxial compressive strength of undrained rock core specimens without pore pressure measurements. In **Annual Book of ASTM Standards** (Vol. 04.08). Philadelphia: American Society for Testing and Materials.

ASTM D2938-95. Standard test method for unconfined compressive strength of intact rock core specimens. In **Annual Book of ASTM Standards** (Vol. 04.08). Philadelphia: American Society for Testing and Materials.

ASTM D3967-95a. Standard test method for splitting tensile strength of intact rock core specimens. In **Annual Book of ASTM Standards** (Vol. 04.08). Philadelphia: American Society for Testing and Materials.

ASTM D4406-93. Standard test method for creep of cylindrical rock core specimens in triaxial compression. In **Annual Book of ASTM Standards** (Vol. 04.08). Philadelphia: American Society for Testing and Materials.

ASTM D5731-95. Standard test method for determination of point load strength index of rock. In **Annual Book of ASTM Standards** (Vol. 04.08) Philadephia: American Society for Testing and Materials.

Aubertin, M. (1996). On the physical origin and modeling of kinematics and isotropic hardeningof salt. In **Proceedings of the Third Conference on the Mechanical Behavior of Salt** (pp. 1-18). Clausthal, Germany: Trans Tech Publications.

Aubertin, M., Gill, D. E., and Ladanyi, B. (1991). A unified visco-plastic model for the inelastic flow of alkali halides. **Mechanics of Materials.** 11: 63-82.

Aubertin, M., Gill, D. E., and Ladanyi, B. (1992). Modeling the transient inelastic flow of rock salt. In **the Seventh Symposuim on Salt** (vol. 1, pp. 93-104). Elsevier Science Pub.

Aubertin, M., Julien M. R., Servant, S., and Gill, D. E. (1999). A rate-dependent model for the ductile behavior of salt rocks. **Canadian Geotechnical Journal.** 36(4): 660-674.

Aubertin, M., Sgaoula, J., and Gill, D. E. (1992). A damage model for rock salt: Application to tertiary creep. In **the Seventh Symposuim on Salt** (vol. 1, pp. 117-125). Elsevier Science Pub.

Aubertin, M., Sgaoula, J., and Gill, D. E. (1993). Constitutive modeling of rock salt: Basic considerations for semi-brittle behavior. In **Proceedings of the Fourth International Symposuim on Plasticity and It's Current Applications** (pp. 92). Baltimore.

Aubertin, M., Sgaoulla, J., Servant, S., Julien, M. R., Gill, D. E., and Ladanyi, B. (1998). An upto-date version of SUVIC-D for modeling the behavior of salt. In **Proceedings of the Fourth Conference on the Mechanical Behavior of Salt** (pp. 205-220). Clausthal,Germany: Trans Tech Publications.

Bagde, M.N., and Petros, V. (2004). Experimental investigation into fatigue behaviour of intact sandstone and conglomerate rock types in uniaxial dynamic cyclic loading. **Geophysical Research Abstracts**, 6: 07240.

Bagde, M.N., and Petros, V. (2005). Fatigue properties of intact sandstone samples subjected to dynamic uniaxial cyclical loading. **International Journal of Rock Mechanics and Mining Sciences**, 42(2): 237-250.

Chokski, A. H., and Langdon, T. G. (1991). Characteristics of creep deformation in ceramics. **Materails Science and Technology** 7: 577-584.

Costin, L.S., and Holcomb, D.J. (1981). Time-dependent failure of rock under cyclic loading. **Tectonophysics**, 79(3-4): 279-296.

Dusseault, M.B., and Fordham, C.J. (1993). Time-dependent behavior of rocks. **Comprehensive Rock Engineering Principles, Practice and Project: Rock Testing and Site Characterization** (Vol. 3, pp. 119-149). London, Pergamon.

Fokker, P. A. (1995). **The behavior of salt and salt caverns**. Ph.D Thesis, Delft University of Technolgoy.

Fokker, P. A. (1998). The micro-mechanics of creep in rock salt. In **Proceedings of the Fourth Conference on the Mechanical Behavior of Salt** (pp. 49-61). Clausthal-Zellerfeld, Germany: Trans Tech Publications.

Fokker, P. A., and Kenter, C. J. (1994). The micro mechanical description of rock salt plasticity. In **Eurock'94** (pp. 705-713). Rotterdam: Balkema.

Franssen, R. C. M., and Spiers, C. J. (1990). Deformation of polycrystalline salt in compression and in shear at 250-350°C. **Deformation Mechanisms, Rheology and Tectonics, Geological Society Special Publication** 45: 201-213.

Fuenkajorn, K., and Phueakphum, D. (2010). Effects of cyclic loading on mechanical properties of Maha Sarakham salt. **Engineering Geology**. 112 (1-4) 43-52.

Fuenkajorn, K., and Daemen, J. J. K. (1988). **Boreholes closure in salt**. Technical Report Prepared for The U.S. Nuclear Regulatory Commission. Report No. NUREG/CR-5243 RW. University of Arizona.

Garcia, E.G., and Estrada, J.H. (1998). Study of correlation between creep tests and variable deviator stress tests in samples of rock salt from Tuzandepetl dome, Veracruz, Mexico. **International Journal of Rock Mechanics and Mining Sciences** (Vol. 35, No. 4/5, pp. 559-562).

Itasca (1992). **User manual for FLAC–fast Langrangian analysis of continua**, **version 3.0**. Itasca Consulting Group Inc., Minneapolis, MN.

Jaeger, J.C., and Cook, N.G.W. (1979). **Fundamentals of rock mechanics (3rd. Edn.).** Chapman and Hall, London, pp. 105-106.

Jandakaew, M. (2003). **Experimental assessment of stress path effects on salt deformation**, M.S. thesis, Suranaree University of Technology, Thailand.

Jeremic, M. L. (1994). **Rock mechanics in salt mining** (530 pp.). Rotherdam: A. A. Balkema.

Knowles, M. K., Borns, D., Fredrich, J., Holcomb, D., Price, R., and Zeuch, D. (1998). Testing the disturbed zone aroud a rigid inclusion in salt. In **Proceedings of the Fourth Conference on the Mechanical Behavior of Salt** (pp. 175-188). Clausthal, Germany: Trans Tech Publications.

Munson, D. E., and Wawersik, W. R. (1993). Constitutive modeling of salt behavior State ofthe technology. In **Proceedings of the Seventh International Congess on Rock Mechanics** (vol. 3, pp. 1797-1810). Balkema.

Passaris, E.K.S. (1982). Fatigue characteristics of rock salt with reference to underground storage caverns. In **Proceedings ISRM Symposium, Rock Mechanics**: Caverns and Pressure Shafts, 26-28 May. Aachen, pp. 983-989.

Raj, S. V., and Pharr, G. M. (1992). Effect of temperature on the formation of creep substructure in sodium chloride single crystal. **American Ceramic Society** 75 (2): 347-352.

Richards, J. (1993). **Plasticity and creep. theory, examples, and problems**. English Edition Editor, Rochester Institute of Technology; Rochester, New York.

Senseny, P. E., Handin, J. W., Hansen, F. D., and Russell, J. E. (1992). Mechanical behavior of rock salt: phenomenology and micro-mechanisms. **International Journal of Rock Mechanics and Mining Sciences** 29 (4): 363-378.

Tepnarong, P. (2001). **Theoretical and experimental studies to determine compressive and tensile strengths of rocks, using modified point load testing**. M.S. Thesis, Suranaree University of Technology, Thailand.

Tepnarong, P. (2006). **Theoretical and experimental studies to determine elastic modulus and triaxial compressive strengths of intact rocks by modified point load testing**. Ph. D. Thesis, Suranaree University of Technology, Thailand.

Thoms, R.L., and Gehle, R. (1982). Experimental study of rock salt for compressed air energy storage. In **ISRM Symposium, Rock Mechanics**: Caverns and Pressure Shafts, 26-28 May 1982. Aachen, pp. 991-1002.

Wang, G. (2004). A new constitutive creep-damage model for salt rock and its characteristics. **International Journal of Rock Mechanics and Mining Sciences** (Vol. 41, No. 3).

Wanten, P. H., Spiers, C. J., and Peach, C. J. (1996). Deformation of NaCl single crystals at 0.27Tm < T < 0.44Tm. In **Proceedings of the Third Conference on the Mechanical Behavior of Salt** (pp. 117-128). Clausthal, Germany: Trans Tech Publications.

Warren, J. (1999). **Evaporites: Their Evolution and Economics** (pp.235-239). Blackwell Science. Oxford

APPENDIX A

TECHNICAL PUBLICATION

TECHNICAL PUBLICATION

Samsri, P., and Fuenkajorn, K. (2009). **Modified point load creep testing of Maha Sarakham rock salt**. In Proceeding EIT-JSCE Joint International Symposium Geotechnical Infrastructure Asset Management. Bangkok, Thailand, 7-8 September 2009.

Modified point load creep testing of Maha Sarakham rock salt

P. Samsri & K. Fuenkajorn
Geomechanics Research Unit, Suranaree University of Technology, Thailand

Keywords: Creep, point load, rock salt, failure, testing

ABSTRACT

An attempt is made to develop a new testing technique, called modified point load creep test (MPL), to determine the time-dependent properties of rock salt. The Middle and Lower salt members of the Maha Sarakham formation are prepared rock disk specimens with diameters of 48 and 101 mm. The applied constant axial stresses are varied from 8 to 24 MPa. The test duration is 30 days. Assuming that Burgers model is valid the elastic, visco-elastic and visco-plastic of the tested salt are calibrated from the test results. Cyclic point loading tests are also performed to determine the true elastic properties of the salt with the axial stress varying from 16 to 32 MPa. The results are compared with those from the cyclic uniaxial tests with the axial stresses varying from 16 to 18 MPa.

1 INTRODUCTION

The modified point load (MPL) testing has been proposed to predict the compressive and tensile strengths and elastic modulus of intact rock specimens in the laboratory (Tepnarong and Fuenkajorn, 2004; Tepnarong, 2006). The test apparatus is similar to that of the conventional point load (CPL) test, except the loading points are cut flat to have a circular cross-sectional area instead of half-spherical shape loading points. The test procedure is intended to be inexpensive, quick and easy while producing results that are comparable to those obtained from the conventional (ASTM) test methods. Much of the MPL testing practices have been concentrated on circular and rectangular disk specimens of soft to medium strong rocks. Test results from rock salt have been rare, and hence are not sufficient to confirm that the MPL testing technique is truly valid or even adequate to determine the basic mechanical properties under a wide range of rock strengths, and on-site where rock drilling and cutting devices are not available.

The objective of this research is to determine salt creep properties by the modified point load testing. The tests are used rock salt from the middle and lower of Maha Sarakarm Formation. The laboratory tests using the relevant ASTM standard practices are carried out to determine the mechanical properties of rock salt in the Maha Sarakham Formation. The creep property parameters are determined from creep testing. The capabilities of the MPL and conventional testing are assessed by comparing the results with those obtained from the conventional methods. Similarity and discrepancies will be discussed.

2 ROCK SALT SPECIMENS

The specimens tested here have been obtained from the Middle and Lower Salt members of the Maha Sarakham formation in the northeastern of Thailand. The rock salt is relatively pure halite with slight amount (less than 1-2%) of anhydrite, clay minerals and ferrous oxide. The average crystal (grain) size is about 5×5×10 mm. Warren (1999) gives detailed descriptions of the salt and geology of the basin.

Sample preparation followed the ASTM (D4543) standard practice, as much as practical. Five specimens (L/D = 2.5) were prepared for uniaxial cyclic loading tests, 10 specimens (t/d = 2-2.5) for modified point load (MPL) cyclic loading tests, and 10 specimens (t/d = 2-2.5) for modified point load (MPL) creep tests. The samples were cut and ground using saturated brine as lubricant. After preparation, the specimens were labeled and wrapped with plastic film. The specimen designation was identified. Prior to mechanical testing, visual examination was made to determine the type and amount of inclusions.

3 UNIAXIAL CYCLIC LOADING TESTS

A series of uniaxial cyclic loading tests have been performed on the 48 mm diameter salt core specimens using a SBEL PLT-75 testing machine (Figure 1). The maximum axial stresses vary among specimens from 16.4 MPa to 18.3 MPa (about 60% to 100% of the compressive strength) while the minimum stress is maintained constant at 0.1 MPa for all specimens. This small minimum stress is required to ensure that the ends of the specimen remain in contact with the loading platens during the test. The loading frequency is 0.3 Hz. The accumulated axial strain, fatigue stress (S) and time are monitored during loading. Some examples of axial stress-strain curves measured during loading are given in Figure 2. Figure 3 shows the decrease of the failure (fatigue) stress as the number of loading cycle (N) increases, which can be represented by a power equation: $S = 20.63\ N^{(-0.033)}$. The behavior is similar to those obtained elsewhere for other geologic materials (Costin & Holcomb, 1981; Thoms & Gehle, 1982; Passaris, 1982; Bagde & Petros, 2004, 2005).

4 CYCLIC MODIFIED POINT LOAD TESTS

The cyclic MPL test is similar to uniaxial cyclic loading test. The MPL tests are performed on salt specimens with thickness-to-loading point diameter ratio (t/d) of 2-2.5 and diameter of specimen-to- loading point diameter ratio (D/d) of 2-4. The MPL loading points used in this study are 10 to 30 mm in diameter. The test apparatus is similar to that of the conventional point load (CPL) test, except the loading points are cut flat to have a circular cross-sectional area instead of half-spherical shape loading points (Figures 4 to Figure 5). Over 10 specimens are prepared for this tested. The loading frequency is 0.3 Hz. Some examples of axial stress-strain curves measured during loading are given in Figure 6. Figure 7 shows comparison between specimen with 48 and 101 diameter decrease of the failure (fatigue) stress as the number of loading cycle (N) increases, which can be represented by power equation. The MPL strength (P_{mpl}) is calculated by:

$$P_{mpl} = p_f / (\pi d^2 / 4) \quad (1)$$

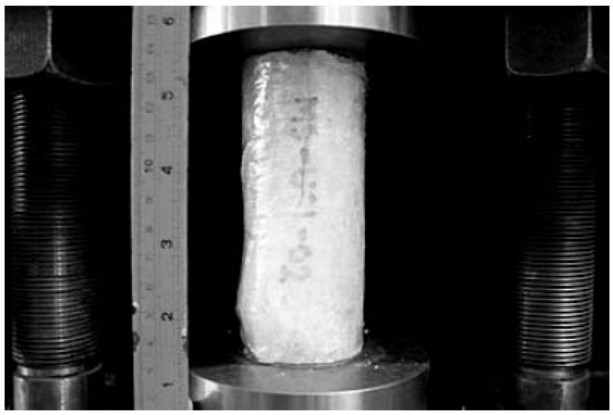

Figure 1. Salt specimen placed in the SBEL PLT-75 testing machine for uniaxial cyclic loading test.

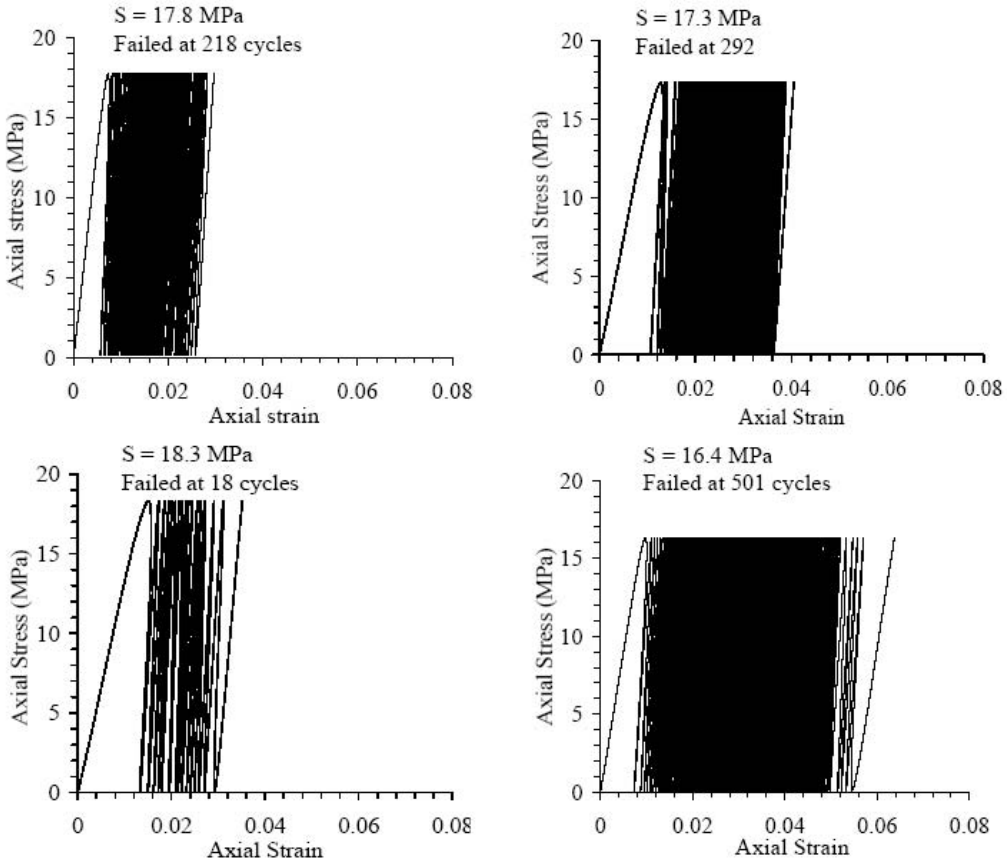

Figure 2. Examples of uniaxial cyclic loading test results. Axial stress plotted as a function of axial strain.

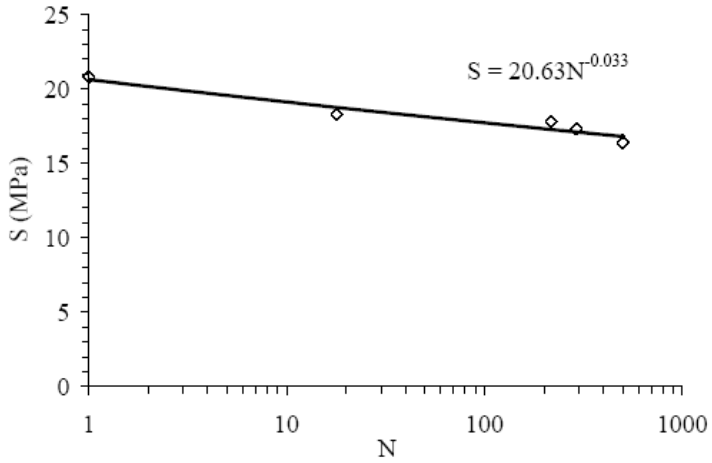

Figure 3. Failure stress (S) plotted as a function of number of loading cycles at failure (N).

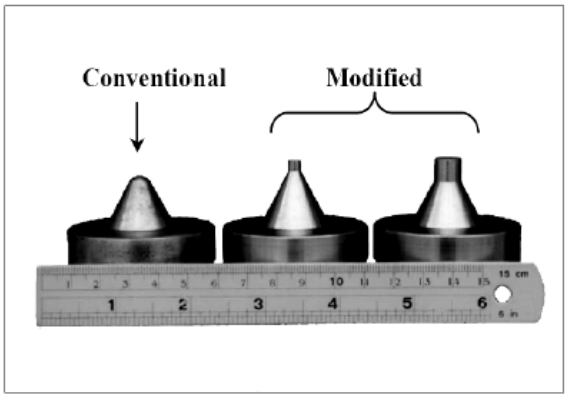

Figure 4. CPL and MPL loading points (Tepnarong, 2001).

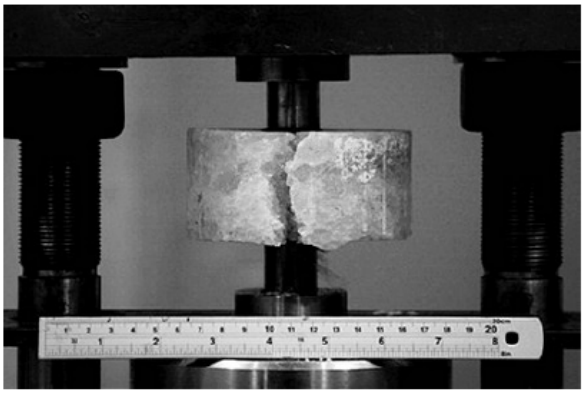

Figure 5. Example salt specimen failed in testing machine for MPL cyclic loading test.

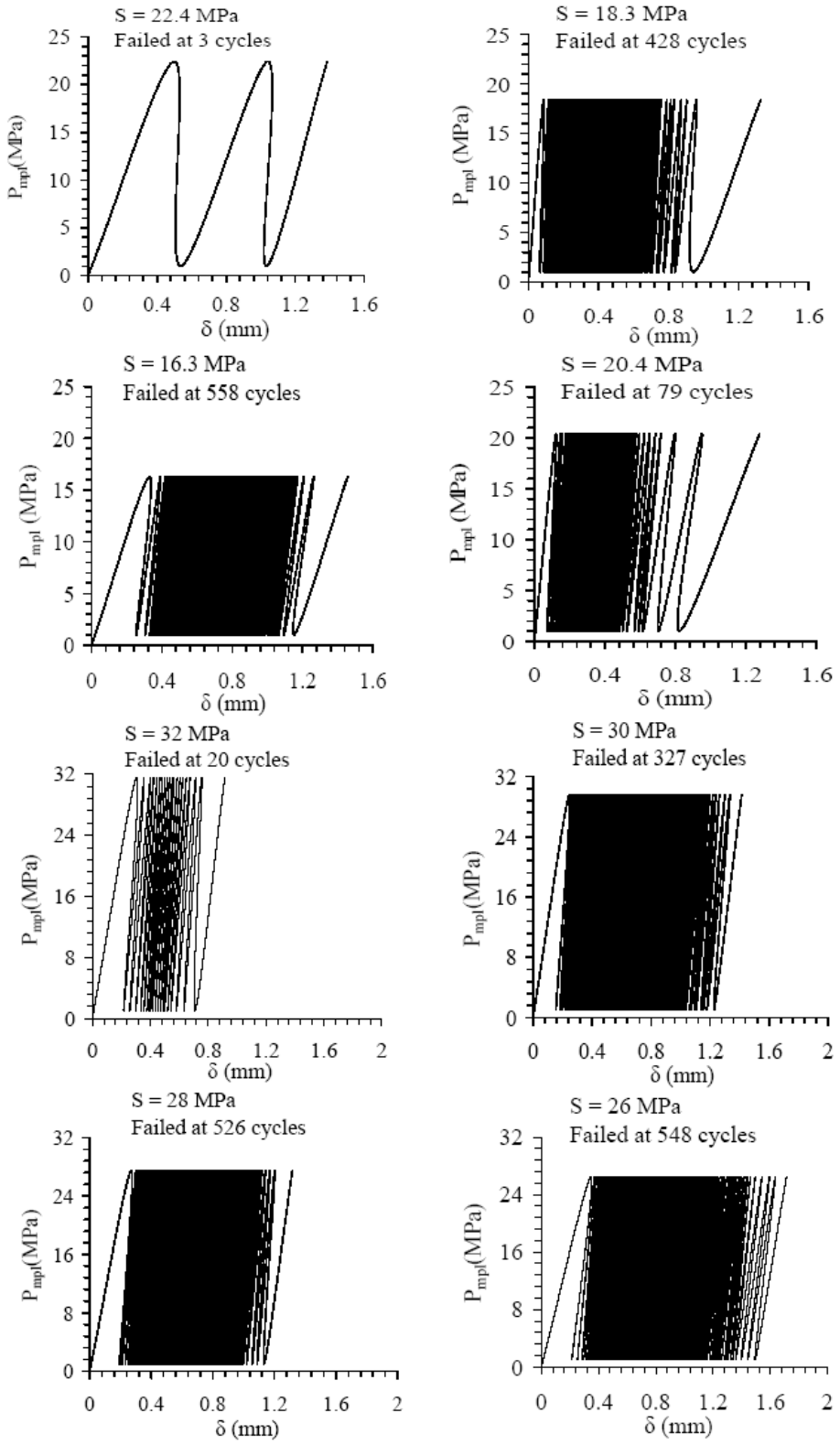

Figure 6. Examples of MPL cyclic loading test results. Axial stress (P_{mpl}) plotted as a function of axial displacement (δ).

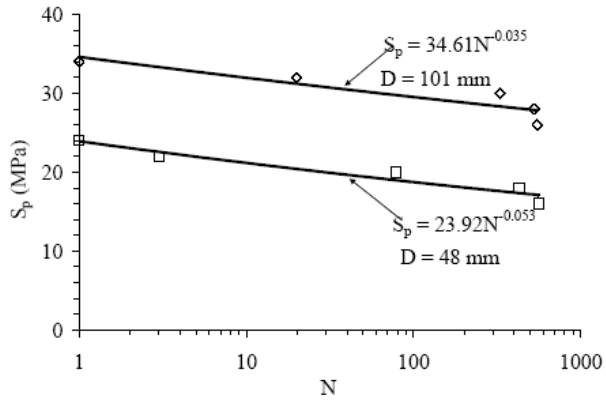

Figure 7. Failure stress (S_p) plotted as a function of number of point loading cycles at failure (N). D indicates the diameter of salt specimens.

5 MODIFIED POINT LOAD CREEP TESTING

The long-term MPL creep tests have been performed to determine the time-dependent properties of the salt under isothermal condition. The test is similar to uniaxial creep test. The long-term results will be used to calibrate the visco-plastic and visco-elastic parameters coefficient of the salt. For the MPL testing, the applied constant axial stresses (P_{mpl}) vary from 8 to 24 MPa. The tests are performed on salt specimens with thickness-to-loading point diameter ratio (t/d) of 2 and 2.5, with diameter of specimen-to-loading point diameter ratio (D/d) of 2 and 4. Some examples of specimen placed in loading machine during loading are given in Figure 8. Figures 9 plots the axial strain as a function of time. Figure 10 shows example of salt specimens after MPL creep tests.

6 SALT PROPERTY CALIBRATION

To assess the effect on the time-dependent properties of salt, a simple rheological creep model is used to describe the constitutive behavior of the salt under isothermal condition. Figures 11 and 12 show the results from the comparison between the calibration and the experimental results for the MPL creep test. These elastic and time-dependent parameters can be calibrated from the laboratory test results using a regression analysis. Tepnarong (2006) proposes an empirical equation to correlate the elastic modulus of MPL specimen with the ratio of the applied load-to-vertical deformation ratio as:

$$E_{mpl} = \left(\frac{T}{\alpha_E}\right)\left(\frac{\Delta P}{\Delta \delta}\right) \qquad (2)$$

where E_{mpl} is elastic modulus predicted by MPL test, α_E is displacement function obtained from numerical analysis, $\Delta P/\Delta\delta$ is the stress change to displacement ratio obtained from unloading curve, and T is the specimen thickness. The displacement function α_E can be defined as: $\alpha_E = 1.50\ (t/d)^{0.64}$ for $D_e/d \geq 10$ (Tepnarong (2006)). The vertical deformation from equation of elastic modulus predicted by MPL for regression analysis as:

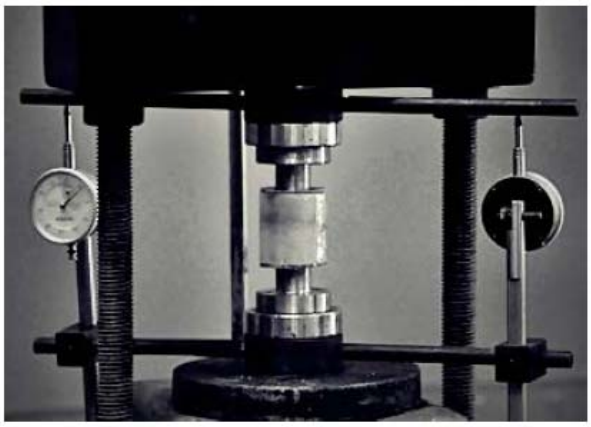

Figure 8. Example salt specimen placed in testing machine for MPL creep test.

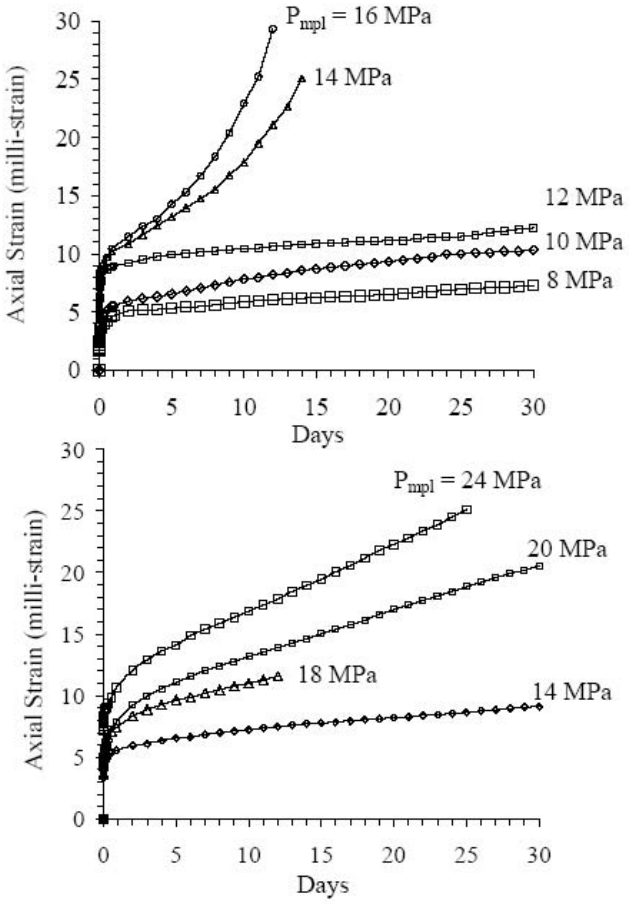

Figure 9. Results of the MPL creep tests with specimens diameters of 48 and 101 mm (from top to bottom).

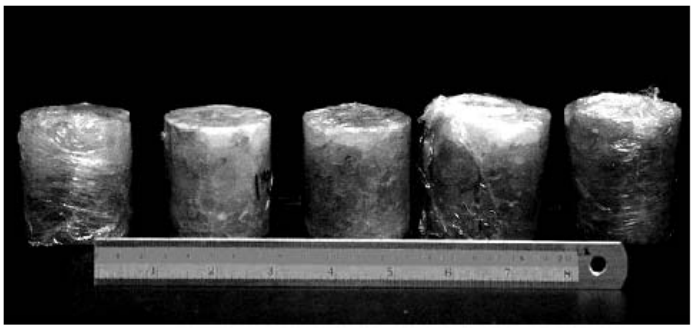

Figure 10. Examples of post-test salt specimens with 48 mm diameter for MPL creep tests.

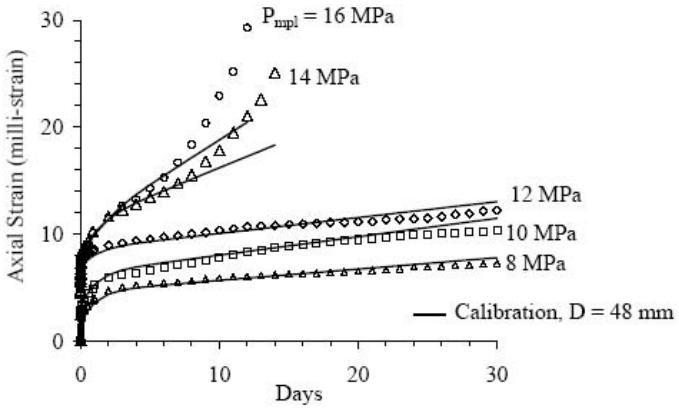

Figure 11. Comparison between the calibration and the experimental results for the MPL creep test with specimens 48 mm diameter.

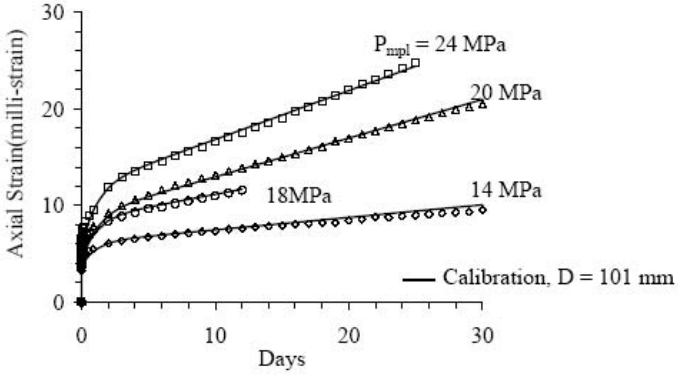

Figure 12. Comparison between the calibration and the experimental results for the MPL creep test with specimens 101 mm diameter.

$$\Delta\delta = \left(\frac{T}{\alpha_E}\right)\left(\frac{\Delta P}{E_{mpl}}\right) \quad (3)$$

The corresponding visco-elastic relation base the Burgers model can be derived as (Richards, 1993):

$$\Delta\delta(t) = \frac{T\Delta P}{\alpha_E}\left[\frac{1}{9K} + \frac{2}{3}\left[\frac{t}{\eta_1} + \left(\frac{1}{E_2} + \frac{(\eta_2 - 1)}{\eta_1 E_2} + \frac{(1+\eta_2)}{E_1}\right)\left(1 - \exp\left(\frac{-E_2 t}{\eta_2}\right)\right)\right]\right] \quad (4)$$

where $\Delta\delta(t)$ is displacement which is a function of time for Burgers model, K is bulk modulus, E_1,E_2 is elastic modulus, and η_1, η_2 is visco-elastic. Tables 1 and 2 summarize the results obtained from the regression analysis.

Table 1. Summary of the property parameters of the salt specimens with 48 mm diameter obtained from calibration.

Test Methods	Axial stress (MPa)	E_1 (GPa)	E_2 (GPa)	η_1 (GPa.day)	η_2 (GPa.day)	K (GPa)
MPL creep test (D = 48 mm)	8	17.0	12.6	43.0	6.5	2.0
	10	21.0	10.0	33.0	3.5	3.3
	12	23.0	20.0	45.0	3.0	6.0
	14	24.0	19.0	15.0	5.0	5.9
	16	25.0	16.0	11.0	5.0	4.3
	Mean±SD	22.0±3.2	15.5±4.2	29.4±15.7	4.6±1.4	4.3±1.7
Uniaxial creep test (D = 48 mm)	Mean±SD	2.6±0.8	2.3±1.2	9.2±5.3	0.8±0.4	3.8±2.0

Table 2. Summary of the property parameters of the salt specimens with 101 mm diameter obtained from calibration.

Test Methods	Axial stress (MPa)	E_1 (GPa)	E_2 (GPa)	η_1 (GPa.day)	η_2 (GPa.day)	K (GPa)
MPL creep test (D =101mm)	14	15.0	9.0	44.0	1.9	3.9
	18	16.0	8.0	33.0	2.0	3.3
	20	19.0	6.5	27.0	1.0	2.2
	24	20.0	6.5	27.0	1.0	3.3
	Mean±SD	17.5±2.4	7.5±1.2	32.8±8.0	1.5±0.6	4.3±1.7
Uniaxial creep test (D = 101 mm)	Mean±SD	4.2±3.5	2.4±2.4	21.0±7.9	2.5±0.4	3.2±2.9

7 DISCUSSIONS AND CONCLUSIONS

The initial results suggest that significant discrepancies exist between the creep parameters obtained from the MPL testing and those from the uniaxial creep testing. This is probably due to the fact that the displacement function α_E suggested by Tepnarong (2006) for hard rocks may not be appropriate for use with soft rock, such as salt. Future effort will be made to derive a new displacement function to obtain a set of the calibrated parameters from MPL creep testing that closer to those obtained from the conventional uniaxial creep testing.

ACKNOWLEDGTMENT

This research is funded by Suranaree University of Technology. Permission to publish this paper is gratefully acknowledged. We would like to thanks Pimai Salt Company for donating salt core for testing.

REFERENCES

ASTM D4543-08. Standard practice for preparing rock core specimens and determining dimensional and shape tolerances. *Annual Book of ASTM Standards,* Vol. 04.08. West Conshohocken, PA: ASTM.

ASTM D7070-08. Creep of rock core under constant stress and temperature. *Annual Book of ASTM Standards*, Vol. 04.08. West Conshohocken, PA: ASTM.

Bagde M.N. & Petros, V., 2004. Experimental investigation into fatigue behaviour of intact sandstone and conglomerate rock types in uniaxial dynamic cyclic loading. *Geophysical Research Abstracts*, 6: 07240.

Bagde, M.N. & Petros, V., 2005. Fatigue properties of intact sandstone samples subjected to dynamic uniaxial cyclical loading. *International Journal of Rock Mechanics and Mining Sciences,* 42(2): 237-250.

Costin, L.S. & Holcomb, D.J., 1981. Time-dependent failure of rock under cyclic loading. *Tectonophysics,* 79(3-4): 279-296.

Passaris, E.K.S., 1982. Fatigue characteristics of rock salt with reference to underground storage caverns. In *Proceeding ISRM Symposium, Rock Mechanics: Caverns and Pressure Shafts, 26-28 May*. Aachen, pp. 983-989.

Phueakphum, D. & Fuenkajorn, K., 2009. Effects of cyclic loading on mechanical properties of Maha Sarakham salt. In *Proceeding second Thailand Symposium, Rock Mechanics: 12-13 March 2009*. Chonburi, Thailand, pp 107-120.

Richards, J., 1993. Plasticity and creep. theory, examples, and problems. English Edition Editor, Rochester Institute of Technology; Rochester, New York.

Tepnarong, P. 2001. Theoretical and experimental studies to determine compressive and tensile strengths of rocks, using modified point load testing. M.S. Thesis, Suranaree University of Technology, Thailand

Tepnarong, P. 2006. Theoretical and experimental studies to determine elastic modulus and triaxial compressive strengths of intact rocks by modified point load testing. Ph.D. Thesis, Suranaree University of Technology, Thailand.

Tepnarong, P. & Fuenkajorn, K., 2004. Determination of elasticity and strengths of intact rocks using modified point load test. *Proceedings of the ISRM International Symposium 3rd ASRM*, Vol. 2 (pp 397-392). Millpress: Rotterdam.

Thoms, R.L. & Gehle, R., 1982. Experimental study of rock salt for compressed air energy storage. In *ISRM Symposium, Rock Mechanics: Caverns and Pressure Shafts, 26-28 May 1982*. Aachen, pp. 991-1002.

Warren, J., 1999, *Evaporites: Their Evolution and Economics*. Blackwell Science. Oxford

BIOGRAPHY

Mr. Pichit Samsri was born on December 3, 1986 in Nakhon Ratchasima province, Thailand. He received his Bachelor's Degree in Engineering (Geotechnology) from Suranaree University of Technology in 2008. For his post-graduate, he continued to study with a Master's degree in the Geological Engineering Program, Institute of Engineering, Suranaree university of Technology. During graduation, 2008-2010, he was a part time worker in position of research assistant at the Geomechanics Research Unit, Institute of Engineering, Suranaree University of Technology. He has published one technical papers related to rock mechanics, titled **"Modified point load creep testing of Maha Sarakham rock salt"** published in the Proceeding of EIT-JSCE Joint International Symposium Geotechnical Infrastructure Asset Management, Bangkok, Thailand.